expression of shNef366 was able to mediate RNAi of *nef* in HeLa-CD4-Nef cells.

Inhibition of HIV-1 replication in U937 cells by lentivirus-based shRNA expression

The transfection efficiency of the entry vectors used in suspension cells was quite low, and the objective here is to introduce siRNAs into primary macrophages. Therefore we constructed HIV-1–based lentivirus vectors expressing Nef366 shRNA or shRNA targeting lacZ as a control (Lenti shNef366 and Lenti control) using Gateway technology. The structure of the lentivirus vector used in the following studies is illustrated in Figure 3A.

To test whether Nef366 shRNA was able to efficiently block HIV-1 replication, we infected U937 cells with Lenti shNef366 or Lenti control, both of which encoded GFP driven by the EF-1α promoter (EGFP), at an MOI of 1. Two weeks after infection, nearly 30% of the cells stably expressed EGFP (Figure 3B upper panel). We sorted the EGFP$^+$ cells by fluorescence-activated cell sorter (FACSaria; BD Biosciences), after which the purity of the Lenti control– and Lenti shNef366–transfected, EGFP$^+$ cells was 97.2% and 99.7%, respectively (Figure 3B lower panel; U937/Lenti cont and U937/Lenti shNef366). The purified cell populations were then infected with 2 inoculation doses of HIV-1 (Figure 3C upper and lower panels; p24: 20 ng and 100 ng, respectively). The culture supernatants were collected at 3- or 4-day intervals, and the level of p24 antigen was measured by ELISA. We observed that at both inoculation doses HIV-1 replication in U937 cells was inhibited by Lenti shNef366, especially at the peak of HIV-1 production. The reverse transcriptase activity was also measured in parallel, and the result was consistent with that of p24 ELISA (data not shown). The inhibition of HIV-1 replication was sustained at least for 1 week, following which HIV-1 production gradually decreased in all cell populations, presumably because of the cytopathic effect of HIV-1 infection.

To further evaluate the effect of RNAi on the early steps of HIV-1 infection, we prepared cell lysates at different time points after inoculation (3, 8, and 12 hours after infection) and analyzed the level of reverse transcription activity by measuring the amount of different forms of proviral DNA (HIV-1 *2LTR* and *U5-Gag*) by the qRT-PCR. The copy number of these proviral DNA forms decreased in U937/Lenti shNef366 cells, relative to that seen in U937/Lenti control cells at all time points. The amount of these DNA forms normalized to β-globin gene at 12 hours after HIV-1 infection is depicted in Figure 3D. The copy number of *2LTR* and *U5-Gag* was 16.9% and 13.4% of control, respectively. These results suggested that the inhibition of HIV-1 replication occurred early after virus entry, presumably during uncoating or reverse transcription, not integration.

A type 1 interferon response has been shown to be induced by synthetic siRNAs via protein kinase R- (PKR) or toll-like receptor 7 (TLR 7)–mediated signaling pathways.[21-23] To eliminate the possibility that we were generating an interferon response following shRNA expression in our system, we analyzed the level of 2′ 5′-oligoadenylate synthetase mRNA expression in Lenti shNef366–infected U937 cells by qRT-PCR. We detected no such message (data not shown), indicating that the interferon response plays a

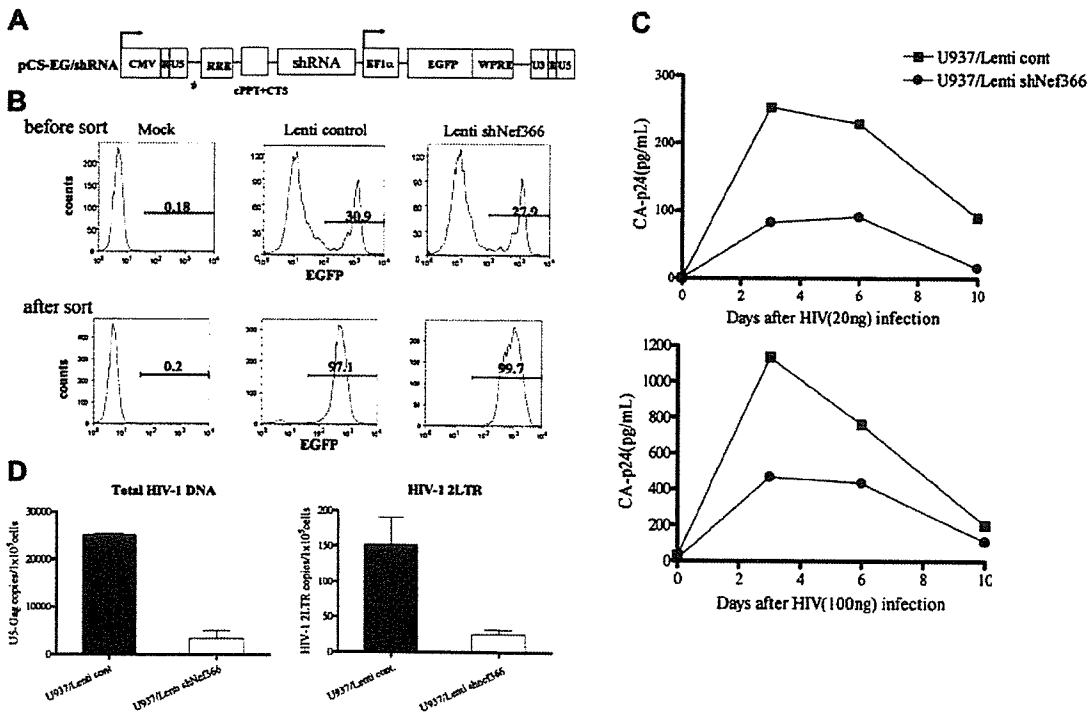

Figure 3. Inhibition of HIV-1 replication in U937 cells by lentivirus-mediated shRNA. (A) The structure of the shRNA lentiviral expression vector. The HIV-1–based lentivirus vector for expressing shRNA was constructed using Gateway technology. pCS-EG/shRNA consisted of U6-shRNA upstream of an EF1α promoter–driven EGFP expression cassette, which allowed simultaneous expression of shRNA and EGFP. (B) U937 cells were infected with lentivirus expressing either shNef366 (Lenti shNef366) or shLacZ (Lenti control) at an MOI of 1. After 2 hours of infection, cells were washed and maintained in culture. Cells expressing EGFP were analyzed by FACS, and EGFP$^+$ cells were collected. EGFP$^+$ cells were analyzed by FACSaria 1 week later (designated as U937/Lenti control and U937/Lenti shNef366). (C) U937/Lenti cont or U937/Lenti shNef366 cells (1 × 10^5/well) were infected with HIV-1_{NL432}, and the culture supernatants of these cells were collected at 3- or 4-day intervals after infection. The level of p24 antigen in the culture supernatants was measured by ELISA. (D) HIV-1–infected cells were collected and total DNA was prepared 12 hours after infection. Total HIV-1 and 2LTR DNA was analyzed by qRT-PCR. The amount of HIV-1–specific DNA per cell was normalized to β-globin gene expression. The data represent the average ± SD of 3 independent experiments.

minimal role, if any, in the observed inhibitory effect on HIV replication by Lenti shNef366.

Lentivirus-based nef shRNA inhibits HIV-1 replication and affects chemokine production in MDMs

Swingler and coworkers reported that HIV-1 Nef expression in macrophages mediated lymphocyte chemotaxis and activation through the induction of MIP-1α and MIP-1β expresion.[8] To determine the effect of Nef expression during HIV-1 infection in MDMs, we infected MDMs with wild-type HIV-1_{NF462} or the corresponding *nef* gene-deletion mutant, HIV-1_{NF462}dNef, and assessed the kinetics of virus replication by p24-specific ELISA. Representative results from 2 donors are shown in Figure 4A. We consistently observed that the level of HIV-1_{NF462} replication was 2- to 6-fold higher than that of HIV-1_{NF462}dNef in MDMs. These results were consistent with those reported by Swingler et al.[9] Although no apparent T-cell damage was observed during cultivation for 3 weeks following HIV-1 infection, the amount of virus production gradually decreased. We analyzed chemokine production in MDMs infected with HIV-1 wild-type and *nef*-deleted HIV-1 at days 10, 14, and 17 after infection. The level of chemokine production in uninfected MDMs varied depending on the donor, but both donors produced a high level of IL-8 and monocyte chemotactic protein-1 (MCP-1), and a low level of MIP-1α and MIP-1β (data not shown). HIV infection per se, independent of the presence or absence of Nef, did not affect this trend, in that the levels of these chemokines, with the exception of MIP-1β, were only slightly affected by HIV infection. Notably, virus replication resulted in an increased production of MIP-1β, which peaked at 14 days after infection, in parallel with the peak of viral replication. Figure 4B shows the results of the analysis of the levels of MIP-1β and MIP-1α in the 2 donors. HIV-1 infection induced a 2-fold increase in the level of MIP-1β compared with mock-infected MDMs. In contrast, infection with Nef-deleted HIV-1 caused a reduction in the level of MIP-1β in the MDMs from both donors, indicating that Nef is responsible for the up-regulation of MIP-1β, but does not affect MIP-1α, MCP-1, or IL-8 production.

To examine whether shRNAs against the U3-overlapping region of *nef* were able to block HIV-1 replication in MDMs, we infected MDMs with Lenti control or Lenti shNef366, at an MOI of 10 or 2 (Figure 5A left and right panels, respectively). After 2 hours of incubation, cells were extensively washed and cultivated overnight, and the following day, they were infected with HIV-1_{NF462}. Culture supernatants were collected every 3 or 4 days and the level of p24 antigen was measured by ELISA. Of note, despite the extensive washing after lentivirus infection, the level of p24 was quite high up to 7 days after HIV-1 infection. We detected a second peak of virus production, which we interpreted as true HIV-1 replication in MDMs transduced with lentiviral vectors expressing shRNAs. In addition, presumably because of the toxic effect of infection by lentivirus pseudotyped with VSV, the level of p24 antigen was lower than that in MDMs infected with HIV-1 virus. Nevertheless, we observed a similar level of inhibition of HIV-1 replication in MDMs by Lenti shNef366 at 2 different doses of infection (Figure 5A), and the inhibition was maintained for at least 3 weeks after HIV-1 infection.

Macrophages can mediate efficient infection of lymphocytes *in trans*,[9,24] suggesting that macrophages serve as a major reservoir and vehicle for HIV-1 dissemination. We were interested in whether the progeny virus produced from MDMs harboring Nef366 shRNA maintained their ability to infect T cells. Supernatants from MDM cells transduced with Lenti control or Lenti shNef366 were collected 10 days after HIV infection, and the level of p24 antigen was measured and used to quantitate the amount of HIV present. These sources of HIV were designated as HIV/Lenti cont or HIV/Lenti shNef366. Using CEMx174 CCR5/LTR-EGFP cells as indicator cells, we estimated the infectivity of HIV/Lenti cont or HIV/Lenti shNef366 by analyzing the number of $EGFP^+$ T cells following infection (Figure 5B). Compared with HIV-1/Lenti cont, HIV-1/Lenti shNef366 had a significant loss of infectivity in $CCR5^+$ T cells. Our results suggested that Lenti shNef366 has the potential to protect HIV-1 dissemination to T cells by HIV-1–infected MDMs

We also examined the level of chemokine production following HIV infection of MDMs transduced with shRNA lentivirus vectors. Although the basal level of MIP-1α and MIP-1β production was slightly increased following lentivirus infection, the level of MIP-1β decreased in Lenti shNef366 cells compared with Lenti control (Figure 5C). The levels of MCP-1 and IL-8 were either unaffected or somewhat restored by Lenti shNef366 (data not shown).

Lentivirus-based nef shRNA protects progression from latent HIV-1 infection to productive infection

Latent HIV-1 infection can be established following provirus integration into the host genome.[25-27] A small number of infected cells re-enter the resting stage, harboring an integrated copy of the HIV-1 genome. These latent HIV-infected cells represent a barrier to successful virus eradication because subsequent cytokine or

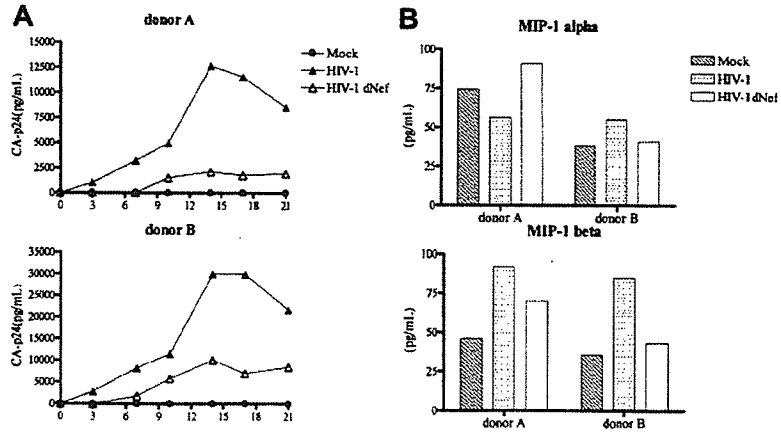

Figure 4. The effect of Nef expression during HIV-1 infection in MDMs. (A) MDMs (2×10^5/well) of 2 donors were infected either with wild-type HIV-1_{NF462} or HIV-$1_{NF462dNef}$. The supernatants of these wells were harvested at 3- or 4-day intervals after infection, and viral production was monitored by sequential quantitation of p24 by ELISA. (B) The CBA kit was used to measure the level of chemokines (MIP-1α and MIP-1β) in cell supernatants 14 days after HIV infection.

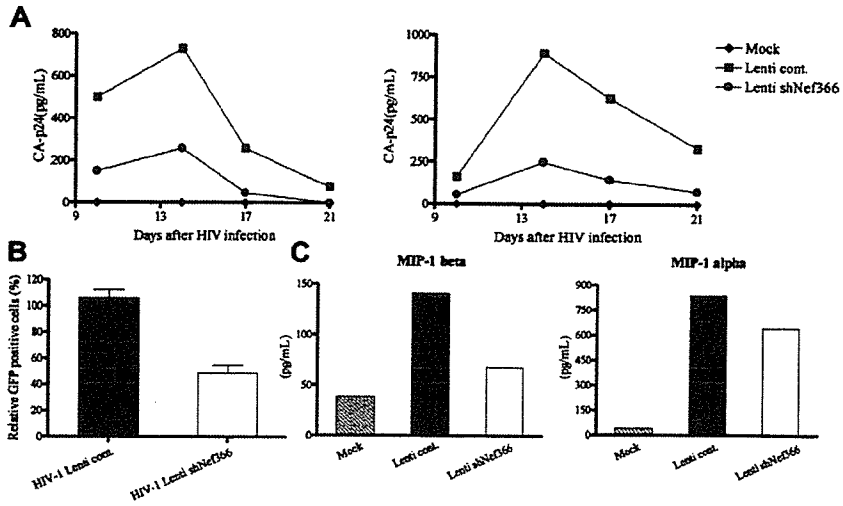

Figure 5. Lentivirus-expressed nef shRNA inhibits HIV-1 replication and affects chemokine production in MDMs. (A) MDMs were transduced with Lenti cont or Lenti shNef366 at an MOI of 2. At 2 hours after infection, cells were washed twice, then cultured for another 24 hours, at which point the cells were infected with HIV-1_{NF462}. The culture supernatants were collected at 3- or 4-day intervals after HIV infection, and the level of p24 antigen was measured by ELISA. (B) MDMs transduced either with Lenti control or Lenti shNef366 were infected with HIV-1 and supernatants were collected 10 days after infection and designated as HIV-1 Lenti cont and HIV-1 Lenti shNef366, respectively. CEMx174 CCR5/LTR-EGFP cells were infected either with HIV-1 Lenti cont or HIV-1 Lenti shNef366 and GFP$^+$, HIV-1–infected T cells were analyzed by FACS 48 hours later. The data represent the average ± SD of 3 independent experiments. (C) The culture supernatants of MDMs transduced with lentivirus vectors were collected 14 days after infection and the levels of the chemokines MIP-1α and MIP-1β were measured.

other stimuli can reactivate viral gene expression, and reinitiate HIV-1 replication.[28-31] We were interested in whether Lenti shNef366 was able to regulate the progression of latent HIV-1 infection to productive infection in U1 cells.[17] U1 cells are U937 cells in which a latent HIV-infection has been established, and HIV-1 replication can be induced in these cells on appropriate activation. We transduced U1 cells with Lenti control or Lenti shNef366 at an MOI of 1. After 2 hours of infection, cells were extensively washed and maintained in culture. Two weeks after transduction, the cells were sorted by FACSaria, and the EGFP$^+$ cell population was stimulated with 1 ng/mL recombinant GM-CSF. Culture supernatants were collected at different time points (days 2 and 5) and the level of p24 antigen was measured by ELISA. As shown in Figure 6, the levels of p24 antigen were dramatically decreased in U1 cells harboring Lenti shNef366 at all time points examined.

Discussion

In this study, we constructed an shRNA expression system that targeted HIV *nef* gene sequences that overlap the 3′ LTR U3 (Nef366) and showed that Nef366 shRNA had a strong inhibitory effect on *nef* gene expression in Nef-expressing HeLa-CD4 cells. Furthermore, expression of shNef366 in monocytic cell lines strongly inhibited the replication of HIV-1 at an early stage of HIV infection. The rational for using shNef366 to target HIV *nef* was several-fold. Because the U3 region is required during reverse transcription for first template transfer and integration of the viral genome into the host genome, siRNA targeting of the U3 region may induce not only specific degradation of *nef* mRNA, but also inhibit HIV-1 reverse transcription. Furthermore, although others have observed escape mutations in RNAi experiments targeting *nef* or *tat*,[32,33] the nef/U3 sequence we targeted is highly conserved as discussed in the paragraph after the next one. If a mutation were to occur in the U3 region, it would affect the overall transcription efficiency of HIV-1 after integration because the U3 region of the HIV-1 LTR contains the transcription initiation or promoter/enhancer sites that are essential for efficient HIV transcription. Of note, the strategy used Jacque et al[20] using siRNA targeting of the 5′ region of *nef* turned out to induce an escape mutant.[33] Although we did not extensively test for the emergence of escape mutants, targeting the 3′ LTR U3-overlapping region of *nef* (Nef366) represented a potentially potent strategy for controlling HIV-1 replication.

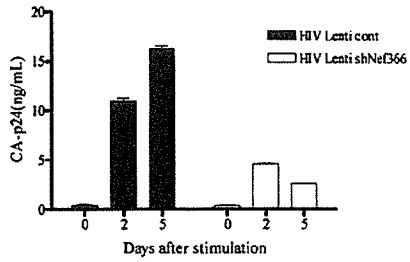

Figure 6. The effect of Lenti shNef366 on latent HIV-1 infection. Latent HIV-1–infected U1 cells were transduced with Lenti control or Lenti shNef366 at an MOI of 1. Two weeks after infection, EGFP$^+$ cells were sorted by FACSaria, and EGFP$^+$ cells were stimulated with 1 ng/mL recombinant GM-CSF. Cell-culture supernatants were collected 0, 2, and 5 days after stimulation, and the level of p24 antigen was measured by ELISA. The data represent the averages ± SDs of 3 independent experiments.

Macrophages are one of the major target cell populations in the early phase of HIV-1 infection, when R5 viruses predominate.[34] HIV-1 replication in macrophages is usually slow and less cytopathic compared with that in activated T cells, allowing the virus to survive long after infection. Thus, macrophages serve as one of the reservoirs for HIV in an infected individual.[35] Therefore, therapeutic strategies that target macrophages are promising approaches to the control of persistent HIV-1 infection in vivo. Taking advantage of the lentivirus expression system, which is an efficient way to introduce a desired gene into primary cells, we were able to show that expression of Nef366 shRNAs in primary MDMs inhibited HIV-1 replication in these cells.

In this context, several groups have demonstrated that RNAi, mediated by the introduction of HIV-specific siRNA duplexes, can inhibit viral replication in T cells, although the effect was transient.[20,36-38] Das et al were able to show a stable inhibitory effect on viral replication using a murine retrovirus vector expressing Nef-specific siRNAs in T cell lines. However, the block in virus replication was not absolute and escape mutants emerged.[33] These previous results prompted us to develop a novel strategy of RNAi-mediated inhibition of HIV infection that did not induce a type 1 interferon and had a stable, long-term effect. We chose to

transduce Nef366 shRNA into low or nondividing primary macrophages, as opposed to actively proliferating T cells, using a lentivirus expression vector, and were able to demonstrate RNAi effect during macrophage cultivation for 3 weeks. Using an alignment of 200 HIV-1 sequences obtained by BLAST search analysis, only one base mismatch in the Nef366 region was detected in a subtype A virus (GenBank no. AB098332 and no. AB098333, HIV-1 UG029). Further study will be required to determine whether this subtype A virus is resistant to shRNA Nef366. Because Nef/LTR is in a completely conserved region, at least among subtype B viruses, this region might have quite an important function for HIV-1 replication. We speculate that if escape mutants were to emerge in the presence of lentiviral-shRNA Nef366, the compensatory mutation would occur outside of this region.

Importantly, using this system, we were also able to demonstrate a decrease in the infectivity of HIV-1 produced from infected MDMs. This attenuation effect is potentially significant because it implies that lentivirus-mediated RNAi may also reduce transmissibility of HIV-1 overall. However, in light of the significant problem of viral escape during chronic HIV infection, it may become necessary to combine multiple sites of siRNAs targeting the *nef-U3* region in the future.

Control of the latent phase of HIV infection is a key issue for effective therapeutic intervention. We demonstrated here that Lenti shNef366 was able to suppress the reactivation of HIV from latently infected cells. The expression of integrated HIV-1 in latently infected cells is controlled at the level of transcription by cellular factors and the viral transactivator Tat, both of which act through the HIV-1 LTR.[39] Transcription of integrated viral RNA is initiated at the R region of the 5′ LTR. The fact that shNef366, which targeted the U3-overlapping region of Nef, was effective in latently infected cells, suggests that shNef366 can directly target cleavage of *nef* mRNAs or total viral RNAs at the 3′ end. Therefore, our lentivirus-based shRNA expression system appears to be able to control both early and latent HIV-1 infection.

MIP-1α and MIP-1β are ligands of the HIV-1 coreceptor, CCR5. Through interaction with the CCR5 receptor, they promote the maturation of Th1 cells.[40,41] Swingler et al reported that MIP-1α and MIP-1β were induced by Nef in macrophages during HIV infection and that culture supernatants derived from Nef-expressing macrophages induced both chemotaxis and activation of resting T lymphocytes, enabling productive HIV-1 infection of those T cells.[8] These and other results have led to a model of HIV infection in which expression of Nef in HIV-infected MDMs enhances the secretion of MIP-1β, which recruits mainly $CCR5^+$ Th1 cells, resulting in the expansion of R5 tropic HIV-1 during macrophage–T-cell interactions. Our results were partially consistent with this model because the degradation of *nef* mRNA expression resulted in the decreased MIP-1β production. Of note, the production of MIP-1α in our system appeared to be unaffected by Nef expression but was induced by lentivirus infection. Because the production of MIP-1α in HIV-infected MDMs was similar to that in uninfected MDMs, it seems likely that MIP-1α production was enhanced by a non–HIV-specific component of the lentivirus expression system, perhaps VSV-G protein. Although the levels of MCP-1 and IL-8 varied depending on the donor and were independent of Nef expression, we cannot rule out the possibility that other unknown chemokines are induced by Nef. Any such dysregulated chemokine production by Nef expression in macrophages might provide an appropriate environment for HIV to establish an efficient infection and dissemination.

In summary, we demonstrated the feasibility of using lentiviral expression vectors to express shRNAs against the U3-overlapping region of *nef* in primary MDMs, as a type of intracellular immunization and potential gene therapy approach against HIV-1. Future development of an AIDS vaccine based on the specific inhibition of viral gene expression combined with existing therapeutic strategies may provide keys to help eradicate HIV.

Acknowledgments

We thank Masayuki Ishige and Rieko Iwaki for their excellent technical assistance.

References

1. Kestler HW 3rd, Ringler DJ, Mori K, et al. Importance of the nef gene for maintenance of high virus loads and for development of AIDS. Cell. 1991;65:651-662.
2. Agopian K, Wei BL, Garcia JV, Gabuzda D. A hydrophobic binding surface on the human immunodeficiency virus type 1 Nef core is critical for association with p21-activated kinase 2. J Virol. 2006;80:3050-3061.
3. Fackler OT, Baur AS. Live and let die: Nef functions beyond HIV replication. Immunity. 2002;16:493-497.
4. Geyer M, Fackler OT, Peterlin BM. Structure–function relationships in HIV-1 Nef. EMBO Rep. 2001;2:580-585.
5. Steffens CM, Hope TJ. Recent advances in the understanding of HIV accessory protein function. AIDS. 2001;15(suppl 5):S21-S26.
6. Na YS, Yoon K, Nam JG, et al. Nef from a primary isolate of human immunodeficiency virus type 1 lacking the EE(155) region shows decreased ability to down-regulate CD4. J Gen Virol. 2004;85:1451-1461.
7. Deacon NJ, Tsykin A, Solomon A, et al. Genomic structure of an attenuated quasi species of HIV-1 from a blood transfusion donor and recipients. Science. 1995;270:988-991.
8. Swingler S, Mann A, Jacque J, et al. HIV-1 Nef mediates lymphocyte chemotaxis and activation by infected macrophages. Nat Med. 1999;5:997-103.
9. Swingler S, Brichacek B, Jacque JM, Ulich C, Zhou J, Stevenson M. HIV-1 Nef intersects the macrophage CD40L signalling pathway to promote resting-cell infection. Nature. 2003;424:213-219.
10. Hannon GJ. RNA interference. Nature. 2002;418:244-251.
11. Coburn GA, Cullen BR. Potent and specific inhibition of human immunodeficiency virus type 1 replication by RNA interference. J Virol. 2002;76:9225-9231.
12. Lee MT, Coburn GA, McClure MO, Cullen BR. Inhibition of human immunodeficiency virus type 1 replication in primary macrophages by using Tat- or CCR5-specific small interfering RNAs expressed from a lentivirus vector. J Virol. 2003;77:11964-11972.
13. Novina CD, Murray MF, Dykxhoorn DM, et al. siRNA-directed inhibition of HIV-1 infection. Nat Med. 2002;8:681-686.
14. Qin XF, An DS, Chen IS, Baltimore D. Inhibiting HIV-1 infection in human T cells by lentiviral-mediated delivery of small interfering RNA against CCR5. Proc Natl Acad Sci U S A. 2003;100:183-188.
15. Song E, Lee SK, Dykxhoorn DM, et al. Sustained small interfering RNA-mediated human immunodeficiency virus type 1 inhibition in primary macrophages. J Virol. 2003;77:7174-7181.
16. Miyoshi H, Blomer U, Takahashi M, Gage FH, Verma IM. Development of a self-inactivating lentivirus vector. J Virol. 1998;72:8150-8157.
17. Folks TM, Justement J, Kinter A, Dinarello CA, Fauci AS. Cytokine-induced expression of HIV-1 in a chronically infected promonocyte cell line. Science. 1987;238:800-802.
18. Tsunetsugu-Yokota Y, Kato T, Yasuda S, et al. Transcriptional regulation of HIV-1 LTR during antigen-dependent activation of primary T cells by dendritic cells. J Leukoc Biol. 2000;67:432-440.
19. Yamamoto N, Tanaka C, Wu Y, et al. Analysis of human immunodeficiency virus type 1 integration by using a specific, sensitive and quantitative assay based on real-time polymerase chain reaction. Virus Genes. 2006;32:105-113.
20. Jacque JM, Triques K, Stevenson M. Modulation of HIV-1 replication by RNA interference. Nature. 2002;418:435-438.
21. Hornung V, Guenthner-Biller M, Bourquin C, et al. Sequence-specific potent induction of IFN-alpha by short interfering RNA in plasmacytoid dendritic cells through TLR7. Nat Med. 2005;11:263-270.
22. Bridge AJ, Pebernard S, Ducraux A, Nicoulaz AL,

Iggo R. Induction of an interferon response by RNAi vectors in mammalian cells. Nat Genet. 2003;34:263-264.

23. Sledz CA, Holko M, de Veer MJ, Silverman RH, Williams BR. Activation of the interferon system by short-interfering RNAs. Nat Cell Biol. 2003;5: 834-839.
24. Carr JM, Hocking H, Li P, Burrell CJ. Rapid and efficient cell-to-cell transmission of human immunodeficiency virus infection from monocyte-derived macrophages to peripheral blood lymphocytes. Virology. 1999;265:319-329.
25. Garcia-Blanco MA, Cullen BR. Molecular basis of latency in pathogenic human viruses. Science. 1991;254:815-820.
26. McCune JM. Viral latency in HIV disease. Cell. 1995;82:183-188.
27. Finzi D, Siliciano RF. Viral dynamics in HIV-1 infection. Cell. 1998;93:665-671.
28. Chun TW, Stuyver L, Mizell SB, et al. Presence of an inducible HIV-1 latent reservoir during highly active antiretroviral therapy. Proc Natl Acad Sci U S A. 1997;94:13193-13197.
29. Finzi D, Hermankova M, Pierson T, et al. Identification of a reservoir for HIV-1 in patients on highly active antiretroviral therapy. Science. 1997; 278:1295-1300.
30. Wong JK, Hezareh M, Gunthard HF, et al. Recovery of replication-competent HIV despite prolonged suppression of plasma viremia. Science. 1997;278:1291-1295.
31. Chun TW, Engel D, Mizell SB, Ehler LA, Fauci AS. Induction of HIV-1 replication in latently infected $CD4^+$ T cells using a combination of cytokines. J Exp Med. 1998;188:83-91.
32. Boden D, Pusch O, Lee F, Tucker L, Ramratnam B. Human immunodeficiency virus type 1 escape from RNA interference. J Virol. 2003;77:11531-11535.
33. Das AT, Brummelkamp TR, Westerhout EM, et al. Human immunodeficiency virus type 1 escapes from RNA interference-mediated inhibition. J Virol. 2004;78:2601-2605.
34. Moore JP, Kitchen SG, Pugach P, Zack JA. The CCR5 and CXCR4 coreceptors—central to understanding the transmission and pathogenesis of human immunodeficiency virus type 1 infection. AIDS Res Hum Retroviruses. 2004;20:111-126.
35. Aquaro S, Calio R, Balzarini J, Bellocchi MC, Garaci E, Perno CF. Macrophages and HIV infection: therapeutical approaches toward this strategic virus reservoir. Antiviral Res. 2002;55:209-225.
36. Capodici J, Kariko K, Weissman D. Inhibition of HIV-1 infection by small interfering RNA-mediated RNA interference. J Immunol. 2002; 169:5196-5201.
37. Dave RS, Pomerantz RJ. Antiviral effects of human immunodeficiency virus type 1-specific small interfering RNAs against targets conserved in select neurotropic viral strains. J Virol. 2004;78: 13687-13696.
38. Stevenson M. Dissecting HIV-1 through RNA interference. Nat Rev Immunol. 2003;3:851-858.
39. Cullen BR. HIV-1 auxiliary proteins: making connections in a dying cell. Cell. 1998;93:685-692.
40. Loetscher P, Uguccioni M, Bordoli L, et al. CCR5 is characteristic of Th1 lymphocytes. Nature. 1998;391:344-345.
41. Luther SA, Cyster JG. Chemokines as regulators of T cell differentiation. Nat Immunol. 2001;2:102-107.

Bacillus anthracis Edema Toxin Acts as an Adjuvant for Mucosal Immune Responses to Nasally Administered Vaccine Antigens[1]

Alexandra Duverger,* Raymond J. Jackson,* Frederick W. van Ginkel,[2]* Romy Fischer,* Angela Tafaro,* Stephen H. Leppla,[‡] Kohtaro Fujihashi,*[†] Hiroshi Kiyono,[†§] Jerry R. McGhee,* and Prosper N. Boyaka[3]*

Anthrax edema toxin (EdTx) is an AB-type toxin that binds to anthrax toxin receptors on target cells via the binding subunit, protective Ag (PA). Edema factor, the enzymatic A subunit of EdTx, is an adenylate cyclase. We found that nasal delivery of EdTx enhanced systemic immunity to nasally coadministered OVA and resulted in high OVA-specific plasma IgA and IgG (mainly IgG1 and IgG2b). The edema factor also enhanced immunity to the binding PA subunit itself and promoted high levels of plasma IgG and IgA responses as well as neutralizing PA Abs. Mice given OVA and EdTx also exhibited both PA- and OVA-specific IgA and IgG Ab responses in saliva as well as IgA Ab responses in vaginal washes. EdTx as adjuvant triggered OVA- and PA-specific $CD4^+$ T cells which secreted IFN-γ and selected Th2-type cytokines. The EdTx up-regulated costimulatory molecule expression by APCs but was less effective than cholera toxin for inducing IL-6 responses either by APCs in vitro or in nasal washes in vivo. Finally, nasally administered EdTx did not target CNS tissues and did not induce IL-1 mRNA responses in the nasopharyngeal-associated lymphoepithelial tissue or in the olfactory bulb epithelium. Thus, EdTx derivatives could represent an alternative to the ganglioside-binding enterotoxin adjuvants and provide new tools for inducing protective immunity to PA-based anthrax vaccines. ***The Journal of Immunology,*** **2006, 176: 1776–1783.**

Bacillus anthracis expresses the protective Ag (PA),[4] the lethal factor (LF), and the edema factor (EF), which combine to form two AB-type toxins (1–3). The combination of PA and EF leads to the formation of anthrax edema toxin (EdTx), while lethal toxin (LeTx) results from the combination of PA and LF. The PA subunit targets cells via the anthrax toxin receptor (ATR) 1, which resembles the tumor endothelial marker 8 (4), and the related ATR2, which is similar to the capillary morphogenesis gene 2 (5). The EF is an adenylate cyclase which increases intracellular cAMP levels (6–8) and induces edema (6). Most previous studies have focused on LeTx-induced death and alterations in APC functions in susceptible macrophages (Mϕ) (9–11) and dendritic cells (12). Anthrax toxin-fusion protein derivatives consisting of PA and the N-terminal domain of LF (LF^{1-254}) have been used to deliver Ags into the cytosol for presentation via MHC class I molecules and induction of CTL responses (13–16). A recent report suggested that PA may not be needed for intracellular delivery of proteins by the LF N-terminal fragment (17). Intradermal coimmunization with a DNA plasmid encoding the N-terminal fragment of LF, which shares homology with the N-terminal fragment of EF, was reported to induce higher anti-PA Ab responses than immunization with a single plasmid encoding PA (18). Although EdTx was reported to induce accumulation of cAMP in lymphocytes (19) and suppress T cell activation (20), little is known about the effect of EdTx on adaptive immune responses.

Cholera toxin (CT) and the related heat labile toxin I (LT-I) of *Escherichia coli* are AB-type toxins made of pentameric-binding B subunits and enzymatic A subunits with ADP-ribosyl transferase activities (21–23). The B subunits of CT and LT-I bind to GM1 gangliosides on target cells (24), while the more promiscuous B subunit of LT-I also exhibits affinity for GM2 and asialo-GM1 (25–27). CT and LT-I are the best described mucosal adjuvants and both promote mucosal secretory IgA (S-IgA) and plasma Ab responses to coadministered vaccine Ags. Unfortunately, the watery diarrhea induced by these toxins precludes their use as oral adjuvants in humans. In addition, major safety concerns relative to the potential of nasal enterotoxins to target CNS tissues have been reported (28, 29). Thus, nasal enterotoxin could damage CNS tissues in large part through their ADP-ribosyl transferase activity following binding of the B subunit to the promiscuous gangliosides expressed on cells of the CNS (30, 31).

We investigated whether an EdTx derivative could act as a mucosal adjuvant like the enterotoxin CT and LT-I, and promote S-IgA and systemic Ab responses to nasally coadministered vaccine

*Department of Microbiology and [†]Department of Pediatric Dentistry, University of Alabama at Birmingham, Birmingham, AL 35294; [‡]Microbial Pathogenesis Section, National Institute of Allergy and Infectious Diseases, National Institutes of Health, Bethesda, MD 20892; and [§]Division of Mucosal Immunology, Department of Microbiology and Immunology, The Institute of Medical Science, University of Tokyo, Tokyo, Japan

Received for publication June 13, 2005. Accepted for publication November 2, 2005.

The costs of publication of this article were defrayed in part by the payment of page charges. This article must therefore be hereby marked *advertisement* in accordance with 18 U.S.C. Section 1734 solely to indicate this fact.

[1] This work was supported by National Institutes of Health Grants AI 43197, AI 18958, DC 04976, DE 12242, and DK 44240.

[2] Current address: College of Veterinary Medicine, Auburn University, AL 36849.

[3] Address correspondence and reprint requests to Dr. Prosper N. Boyaka, Department of Microbiology, University of Alabama at Birmingham, 772 Bevill Biomedical Research Building, 845 19th Street South, Birmingham, AL 35294-2170. E-mail address: prosper@uab.edu

[4] Abbreviations used in this paper: PA, protective Ag; LF, lethal factor; EF, edema factor; EdTx, anthrax edema toxin; LeTx, lethal toxin; ATR, anthrax toxin receptor; CT, cholera toxin; LT-I, heat labile toxin-I; S-IgA, secretory IgA; CLN, cervical lymph node; RLU, relative light unit; ON/E, olfactory nerves and epithelium; OB, olfactory bulb; Mϕ, macrophage; NALT, nasopharyngeal-associated lymphoepithelial tissue; CP, crossing point.

0022-1767/06/$02.00

Ags. We also queried whether this regimen would enhance immunity to the binding B subunit PA itself and perhaps provide an extra bonus for anthrax immunity. We further examined whether the receptor specificity of EdTx would lead to the accumulation of this toxin into CNS tissues after nasal delivery.

Materials and Methods

Mice

Female C57BL/6 mice, 6–7 wk of age, were obtained from Charles River Laboratories and were 9–12 wk of age when used in these experiments. All studies were performed in accordance with both National Institutes of Health and University of Alabama at Birmingham institutional guidelines to avoid pain and distress.

Immunization

Mice were nasally immunized three times at weekly intervals with 100 μg of OVA (Sigma-Aldrich) alone, OVA plus 5 μg of rPA only, or OVA plus EdTx (5 μg of rPA together with 5 μg of rEF). The rPA was purified from cultures of a recombinant strain of *B. anthracis* as previously described (32). The EF was obtained from List Biological Laboratories (product no. 173) and was produced in a recombinant strain of *B. anthracis* using an expression plasmid constructed by S. H. Leppla. This EF protein contains a S447N mutation and was shown to display ~20-fold less enzymatic activity than the native EF (33). Controls included mice nasally immunized with OVA plus 1 μg of CT (List Biological Laboratories). Mice were lightly anesthetized and given 12.5 μl of vaccine/nostril. Blood and external secretions (fecal extracts, vaginal washes, and saliva) were collected as previously described (34, 35).

Evaluation of OVA- and PA-specific Ab isotypes and IgG subclass responses

Previously described ELISA was used to assess anti-OVA and anti-PA Ab levels in plasma and external secretions (34, 35). Briefly, microtiter plates were coated with OVA (1 mg/ml) or PA (5 μg/ml). The IgM, IgG, or IgA Abs were detected with HRP-conjugated goat anti-mouse μ-, γ-, or α-H-chain-specific antisera (Southern Biotechnology Associates). Biotin-conjugated rat anti-mouse IgG1 (clone A85-1; 0.5 μg/ml), IgG2a (clone R19-15; 0.5 μg/ml), IgG2b (clone R12-3; 0.5 μg/ml), or IgG3 (clone R40-82; 0.5 μg/ml) mAbs and HRP-conjugated streptavidin (BD Pharmingen) were used to measure IgG subclass responses. The color was developed with the addition of ABTS substrate (Sigma-Aldrich), and the absorbance was measured at 415 nm. End-point titers were expressed as the $\log_2$ dilution giving an OD_{415} of ≥ 0.1 above those obtained with nonimmunized control mouse samples.

Total and Ag-specific IgE Abs

Total IgE Ab levels were determined by a BD OptEIA Set Mouse IgE (BD Pharmingen), according to instructions from the manufacturer. To prevent interference in the assay, serial dilutions of immune plasma were previously depleted of IgG by overnight incubation in Reacti-Bind Protein G-Coated Plates (Pierce). To detect Ag-specific IgE, the microtiter plates were coated with OVA (1 mg/ml) or PA (5 μg/ml). Serial dilutions of plasma were then added, IgE was detected with the biotinylated anti-mouse IgE Abs, and titers were determined as described above.

Macrophage toxicity assay to assess anti-PA-neutralizing Abs

The protective effects of PA-specific Abs were determined using a previously described assay (35) that measures their capacity to protect the J774 Mϕ cell line from LeTx (9, 11). Briefly, J774 Mϕ (5×10^4 Mϕ/well) were added to 96-well, flat-bottom plates. After 12 h of incubation, plasma or external secretions samples were added together with LeTx (400 ng/ml PA plus 40 ng/ml LF) and incubated for an additional 12 h as described elsewhere (31). Viable Mϕ were evaluated after addition of MTT (Sigma-Aldrich) (36).

Effect of EdTx on APCs in vitro

J774 Mϕ (5×10^4 cells/ml) or freshly isolated mesenteric lymph node or spleen cells from C57BL/6 mice were incubated in the presence of PA only (5 μg/ml), EF only (5 μg/ml), EdTx (PA + EF; 5 μg/ml), or CT (1 μg/ml). Forty-eight hours later, culture supernatants were collected for evaluation of cytokine responses. Cells were collected and stained for 30 min at 4°C with FITC- or PE-conjugated mAbs (BD Pharmingen). After three washing steps and fixation in 2% paraformaldehyde, the expression of activation and costimulatory molecules was analyzed by flow cytometry.

In vitro restimulation of Ag-specific $CD4^+$ T cells and cytokine-specific ELISA

T cells were isolated from spleen and cervical lymph nodes (CLNs) and restimulated in vitro as previously described (34, 35, 37) with OVA (1 mg/ml) or PA (20 μg/ml) in RPMI 1640 medium containing 10 mM HEPES, 2 mM L-glutamine, 100 U/ml penicillin, and 100 μg/ml streptomycin, 5×10^{-5} M 2-ME, 1 mM sodium pyruvate, and 10% FCS. The Th1 and Th2 cytokines in culture supernatants were determined by cytokine-specific ELISA as previously described (34, 35, 38). The mAb couples were from BD Pharmingen. Standard curves were generated using murine rIFN-γ, rIL-5, rIL-6, and rIL-10, rIL-12 (R&D Systems); rIL-2 and rIL-13 (BD Pharmingen); and rIL-4 (Pierce). The ELISAs were capable of detecting 5 pg/ml for IL-2, IL-4, and IL-5; 15 pg/ml for IFN-γ; 50 pg/ml for IL-13; 100 pg/ml for IL-6, IL-12; and 200 pg/ml for IL-10.

Tracking studies

The PA and CT were labeled with acridinium using an acridinium C_2 NHS ester labeling kit (Assay Designs). The specific activity of PA and CT used in the tracking studies were 2.11×10^7 relative light units (RLU)/ng and 2.06×10^7 RLU/ng, respectively. Mice were given the acridinium-labeled compounds by instilling 5-μl quantities into each nare. Twelve and 24 h following immunization, mice were sacrificed and the olfactory nerves and epithelium (ON/E), olfactory bulbs (OB) and brain (B) were removed as previously described (30). Each tissue was weighed and 200 μl of Cellytic MT lysis buffer (Sigma-Aldrich) was added per 10 mg wet weight of tissue. The ice-cold tissues were homogenized (20,000 rpm for 15–20 s) using a Tissue Tearor (Biospec Products) and frozen at −20°C. After thawing, the homogenates were centrifuged at $10{,}000 \times g$ for 10 min and the supernatants were tested for light activity in triplicate in 96-well Microlite 2 plates (Thermo Labsystems). Nonimmunized mouse tissues served as controls.

Nasal EdTx-induced cytokine responses in vivo

Mice were given PBS, EdTx or CT by instilling 5-μl quantities into each nare. Twelve and 24 h later, mice were sacrificed and nasal washes were collected in 500 μl of PBS and the cytokine content was analyzed by ELISA. The nasopharyngeal-associated lymphoepithelial tissue (NALT), CLN, ON/E, and OBs were removed and subjected to real time RT-PCR (Lightcycler; Roche). The cytokine mRNA levels are expressed as crossing points (CP) or the cycle at which the fluorescence rises appreciably above the background fluorescence as determined by the Second Derivative Maximum Method (Roche Molecular Biochemicals LightCycler Software). The formula mRNA = $2^{(-(CP_{cytokine} - CP_{\beta\text{-}actin}))}$ corrects for differences in cDNA concentration between the starting templates of cytokine and housekeeping (i.e., β-actin) genes (39). The simplified formula $20 - (CP_{cytokine} - CP_{\beta\text{-}actin})$ was used to express relative cytokine mRNA responses in tissues of mice given nasal EdTx.

Statistics

The results are expressed as the mean ± 1 SD. Statistical significance (*, $p \leq 0.05$) was determined by Student's t test and by ANOVA followed by the Fisher least significant difference test. For statistical analysis, cytokine levels below the detection limit were recorded as one-half the detection limit (e.g., IFN-γ = 7.5 pg/ml).

Results

EdTx promotes plasma Ab responses to nasally coadministered Ags

We first examined whether the adenyl cyclase EdTx, which acts through the ATR, would enhance Ab responses to mucosally administered protein Ags. Coadministration with 1 μg of EdTx (1 μg of PA and 1 μg of EF) enhanced OVA-specific plasma IgG Ab responses (Fig. 1*A*). Higher Ab responses were seen in mice given OVA and 5 μg of PA and 5 μg of EF although the titers failed to reach the statistical difference (Fig. 1*A*). The binding of EdTx to its receptor alone did not significantly contribute to the observed adjuvant activity, because neither PA alone (Fig. 1*B*) nor EF alone (data not shown) significantly increased OVA-specific IgG or promoted OVA-specific IgA Ab responses. Coimmunization with PA and EF (i.e., EdTx) sharply increased OVA-specific IgG and induced high levels of IgA Abs (Fig. 1*B*). The EdTx-induced IgG subclass responses consisted mainly of IgG1 and IgG2b Abs (Fig. 1*C*). Plasma samples collected 1 wk after two nasal immunizations

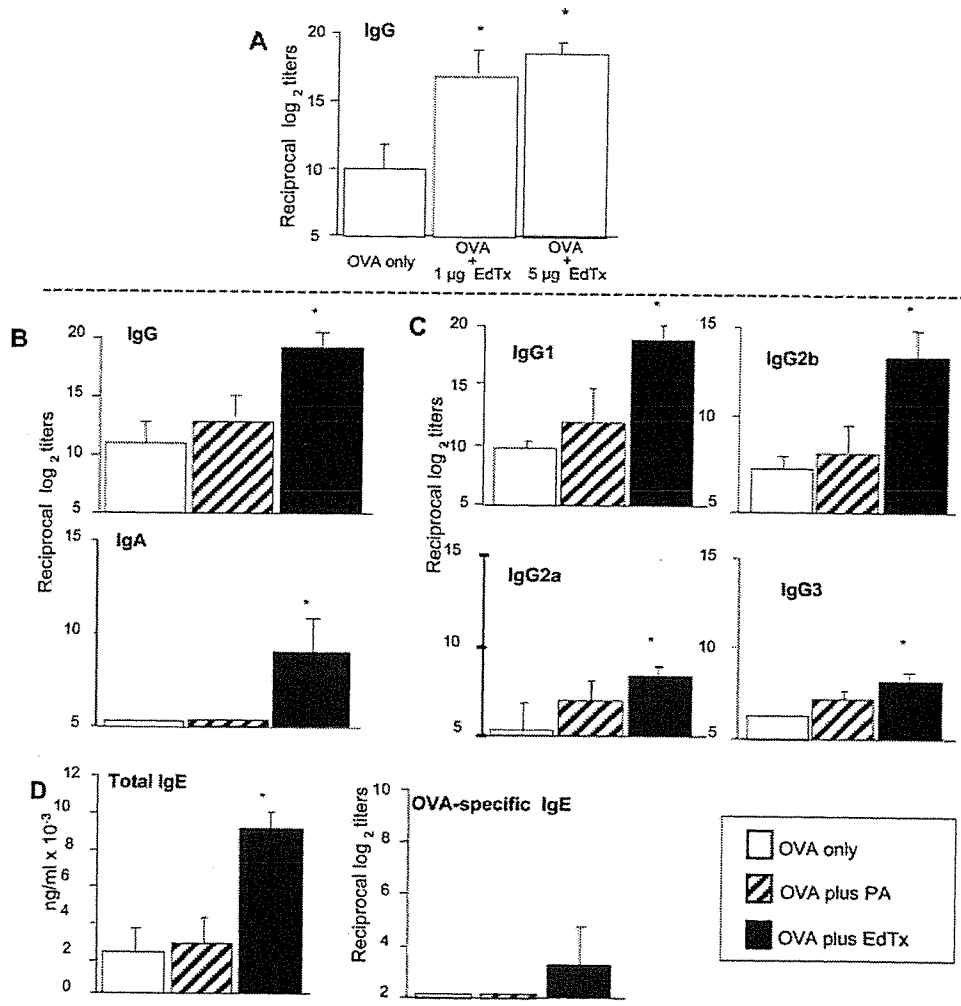

FIGURE 1. Adjuvant effect of EdTx for nasally coadministered Ag. *A*, Effect of EdTx dose on OVA-specific Ab responses. Mice were immunized three times at weekly intervals with 100 μg of OVA only or OVA plus 1 or 5 μg of EdTx (5 μg of PA plus 5 μg of EF). *B*, Role of EdTx component in the adjuvanticity. *C*, Plasma levels of OVA-specific IgG subclass Abs were determined 1 wk after the last immunization. *D*, Plasma samples were collected 1 wk after the second immunization (day 14) and examined for their content of total and OVA-specific IgE Ab levels. Mice were immunized three times at weekly intervals with 100 μg of OVA only (□), OVA plus 5 μg of PA (▨), or OVA plus 5 μg of EdTx (5 μg of PA plus 5 μg of EF) (■). Plasma levels of OVA-specific Abs were determined 1 wk after the last immunization. The results are expressed as the reciprocal $\log_2$ titers ± one SD and are from three (*A*) or five experiments (*B–D*) and four mice/group. *, $p < 0.05$.

with OVA and EdTx contained elevated levels of total IgE Abs and low but significant OVA-specific IgE Abs that were not detected in mice nasally immunized with OVA only or OVA plus PA (Fig. 1*D*).

EdTx enhances PA-specific plasma Ab responses

In addition to acting as adjuvants for mucosally coadministered Ags, CT and LT-I are good immunogens that induce high Ab responses to their respective cell ganglioside-binding B subunits (40–43). Thus, we next addressed whether EdTx could enhance immunity to its binding PA subunit. Low levels of PA-specific IgG and IgA Abs were seen in the plasma of mice that received 5 μg of PA. Interestingly, PA-specific IgG and IgA Ab responses were both significantly increased in mice given EdTx (5 μg of PA plus 5 μg of EF), indicating that the enzymatic EF subunit also enhanced PA-specific Ab responses (Fig. 2*A*). PA-specific IgE Abs were not detected in mice that received PA without EF. However, coadministration of EF induced PA-specific IgE Ab levels (Fig. 2*A*), which were significantly higher than OVA-specific Abs in the same mice (Fig. 1*C*). The EdTx-induced PA-specific IgG subclass responses also predominantly consisted of IgG1 and IgG2b Abs followed by IgG2a and IgG3 (Fig. 2*B*).

EdTx induces PA- and OVA-specific Abs in saliva and vaginal secretions

Because nasal administration of EdTx enhanced systemic Ab responses to both the coadministered protein (i.e., OVA) and the binding B subunit (i.e., PA) itself, we next ascertained whether EdTx also induced PA- and OVA-specific IgA and IgG Abs in saliva and mucosal IgA Ab responses in other external secretions. OVA-specific IgA Abs were not detected in the saliva or the vaginal secretions of mice given OVA only or OVA plus PA (Fig. 3*A*). In contrast, the saliva of mice that received EdTx exhibited both OVA- and PA-specific IgA and IgG Abs (Fig. 3*A*). In addition, PA- and OVA-specific IgA Abs were detected in the vaginal washes of mice immunized with OVA plus EdTx (Fig. 3*B*).

Previous studies have shown that CT as a nasal adjuvant could induce a broad mucosal Ab response with PA-specific IgA Abs in the oral cavity (saliva), gastrointestinal (fecal extracts), and genitourinary (vaginal washes) tracts (35). In contrast to CT, the adjuvant activity of EdTx failed to induce high OVA-specific IgA Abs in fecal extracts (Fig. 3*C*). High amounts of PA (i.e., 40 μg) were needed for CT as a nasal adjuvant to induce anti-PA IgA Abs in fecal extracts (35). Increasing the dose of PA to 40 μg failed to enhance PA- or OVA-specific IgA Abs in fecal extracts (data not shown), suggesting that different mechanisms are involved in the mucosal adjuvanticity of CT when compared with EdTx.

EdTx induces anti-PA-neutralizing Abs

Nasal immunization with OVA and PA resulted in low levels of neutralizing Abs that were seen only in the plasma (Table I). Mice immunized with OVA and EdTx exhibited significantly higher titers of neutralizing Abs in the plasma than mice immunized with OVA plus PA (Table I). More interestingly, saliva of mice given

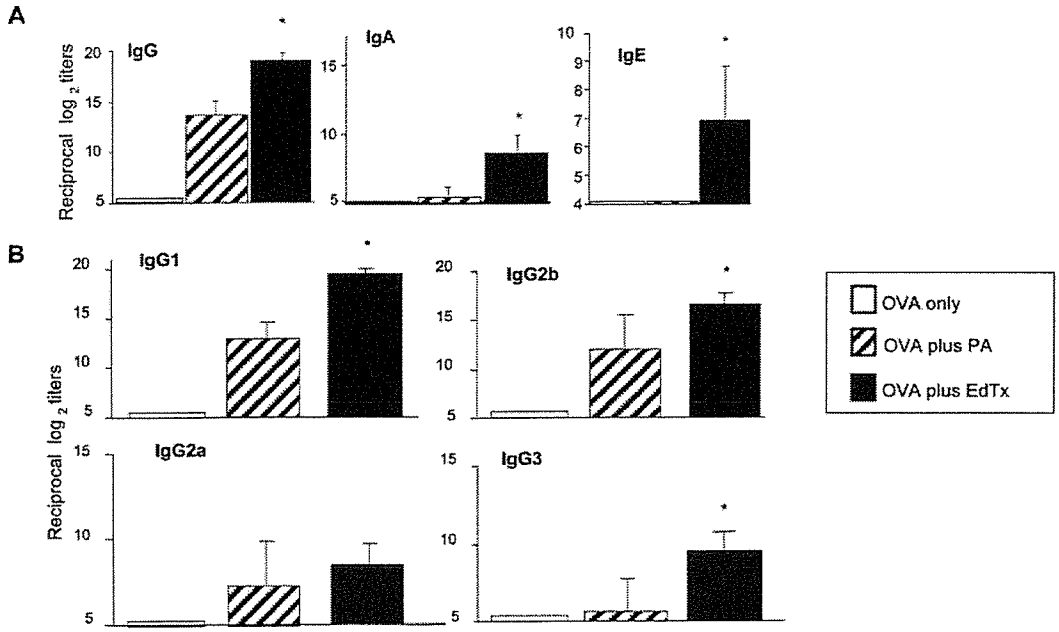

FIGURE 2. Plasma PA-specific Ab responses following nasal immunization with EdTx as adjuvant. Mice were immunized three times at weekly intervals with 100 μg of OVA only (□), OVA plus 5 μg of PA (▨), or OVA plus 5 μg of EdTx (5 μg of PA plus 5 μg of EF) (■). Plasma PA-specific IgE Ab responses were determined in samples collected at day 14, and plasma PA-specific Ab isotype (*A*) and IgG subclass responses (*B*) were determined 1 wk after the last immunization. The results are expressed as the reciprocal $\log_2$ titer ± one SD from five separate experiments and four mice per group per experiment. *, $p < 0.05$

OVA and EdTx contained significant levels of anti-PA neutralizing Abs (Table I). No significant neutralizing Abs were detected in vaginal washes (Table I).

Ag-specific T cell cytokine responses following nasal immunization with EdTx as adjuvant

To characterize $CD4^+$ Th cell cytokine pathways associated with EdTx-induced immunity, we examined the pattern of cytokines secreted by OVA- and PA-specific $CD4^+$ T cell after a 5-day in vitro restimulation. Spleen $CD4^+$ T cells from mice immunized with OVA and EdTx secreted mixed Th1- and Th2-type cytokines after in vitro restimulation with OVA or PA as indicated by high levels of IFN-γ (Th1) but also IL-5, IL-6, and IL-13 in culture supernatants (Table II). IL-4 levels were below the limit of detection. The same profile of cytokine responses was seen in the culture supernatant of CLN $CD4^+$ T cells restimulated under the same conditions (data not shown).

Effect of EdTx on cytokine secretion and costimulatory molecule expression by Mϕ, in vitro

We assessed the direct effects of EdTx or CT on the expression of costimulatory molecules (i.e., CD40 and CD86) as well as cytokine secretion by J774 Mϕ to address whether EdTx regulates APC functions. Consistent with previous reports (44–46), CT induced high levels of IL-6 responses in treated cells (Fig. 4*A*) and increased costimulatory molecule expression (Fig. 4*B*) by Mϕ in vitro. The IL-6 responses after EdTx stimulation were ~10-fold lower than those measured in culture supernatants of J774 Mϕ cultured in the presence of CT (Fig. 4). However, EdTx up-regulated the expression of both CD40 and CD86 by J774 Mϕ to the same extent as the mucosal adjuvant CT. These findings were further confirmed on T cell-depleted spleen cells (data not shown).

Nasal PA does not target CNS tissues

We next explored the possibility that EdTx could target the ON/E or other CNS tissues and induce inflammatory responses. Fig. 5*A*

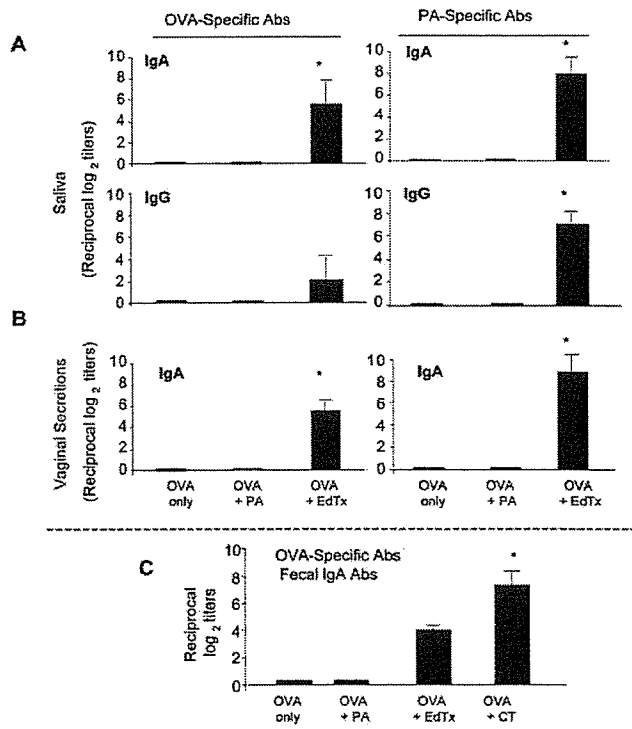

FIGURE 3. Mucosal IgA Ab responses following nasal immunization with EdTx as adjuvant. Mice were immunized three times at weekly intervals with 100 μg of OVA only, OVA plus 5 μg of PA, or OVA plus 5 μg of EdTx (5 μg of PA plus 5 μg of EF). Saliva (*A*) and vaginal washes (*B*) were collected 2 wk after the last immunization. The Ab levels are expressed as the reciprocal $\log_2$ titer ± 1 SD from five separate experiments and four mice per group per experiment. Fecal extracts (*C*) were collected 2 wk after the last immunization with either OVA only, OVA plus PA, OVA plus EdTx, or OVA plus CT. The IgA Ab levels were expressed as the reciprocal $\log_2$ titer ± 1 SD from three separate experiments and four mice per group per experiment. *, $p < 0.05$

Table I. *Neutralizing anti-PA Abs produced in response to nasal administration of EdTx protect Mϕ against the lethal effect of LeTx in vitro*[a]

Immunization	Neutralizing Ab Titers (1/Dilution)		
	Plasma	Saliva	Vaginal Washes
OVA only	BD	BD	BD
OVA plus PA	8,192 ± 256*	BD	BD
OVA plus EdTx	131,072 ± 1,024*	10 ± 3*	3 ± 2

[a] Serial dilutions of each sample were added to J774 Mϕ cultures in the presence of LeTx. The neutralizing titers were determined as the last dilution yielding an MTT OD equal to twice the background value. Results are shown as neutralizing Ab titers and are expressed as the reciprocal dilutions titers ± 1 SE of three separate experiments and five mice per group per experiment. BD, Below detection level; *, $p < 0.05$.

illustrates the failure of PA to accumulate in the ON/E 24 h following nasal delivery of 5 μg of PA. In addition, there was no PA detectable in the OBs or brain and only minor amounts (< 0.15 ng/10 mg tissue) were observed in the NALT, CLN, or spleen 24 h after nasal delivery (data not shown). Nasal PA given together with EF (EdTx) did not increase PA accumulation in olfactory or brain tissues (Fig. 5*A*). In contrast to PA or EdTx, nasal delivery of a 0.5-μg dose of CT resulted in significant accumulation in the ON/E which was further increased when the CT dose was 10-fold higher (Fig. 5*A*). We also found that nasal CT, but not EdTx, up-regulated IL-1 mRNA levels in the ON/E and in the NALT suggesting that CT targeted these two sites (Fig. 5*B*). Finally, mice given nasal CT, but not those given nasal EdTx, exhibited high levels of IL-6 in nasal washes (Fig. 5*C*).

Discussion

The enterotoxins CT and LT-1, which deliver their ADP ribosyl transferase A subunit via ganglioside targeting, are well-recognized adjuvants for induction of mucosal immunity to coadministered Ags (40–42). The CTA1-DD molecule which targets CT-A to B cells was also shown to be an effective mucosal adjuvant (31, 47, 48). EdTx delivers its adenylate cyclase EF subunit into target cells following binding of PA on its membrane receptors, the ATRs. It has been recently reported that ATR1/TEM8 is expressed by epithelial cells (49). However, previous studies have shown that PA binds more effectively to the basolateral membrane of polarized epithelial cells (50), suggesting that ATRs may not be expressed at the apical membrane of these cells. In this study, we show that EdTx promotes both systemic and mucosal adaptive immunity to nasally coadministered Ags and enhances PA-specific Ab responses significantly above levels achieved by administration of PA without EF. We also show that ATR targeting by EdTx did not lead to the accumulation of this adjuvant into olfactory and CNS tissues.

Anthrax toxin derivatives have been evaluated as molecular syringes for intracellular delivery of peptides (13, 51) or protein Ags (14–16) for presentation via the MHC class I pathway and induction of cytotoxic $CD8^+$ T cells. Our results show that in vivo delivery of anthrax EdTx provides necessary signals for induction of mucosal and systemic immunity to coadministered protein Ags. Although data summarized in this manuscript only referred to nasal delivery of EdTx, we also found that EdTx is an adjuvant for protein Ags coinjected i.p. in both C57BL/6 and BALB/c mice (data not shown). Studies with the ganglioside-targeting enterotoxins CT and LT-I (52–55) and derivatives including their chimeras (34, 56) or the B cell-targeting CTA1-DD (31, 57) have demonstrated the importance of receptor binding for controlling the immune responses induced by these ADP-ribosylating adjuvants. Thus, the adjuvant activity of CT appears to be more dependent on IL-4 and $CD4^+$ Th2 cell cytokines (52, 53). In contrast, the more promiscuous LT-I, which binds GM1 gangliosides like CT but also asialo-GM1 and -GM2 gangliosides, promotes a broader spectrum of responses with $CD4^+$ Th cells producing both IFN-γ and Th2-type cytokines (34, 54). The adjuvant activity of nasal EdTx appears to involve Ab and T cells responses that resemble those induced by LT-I rather than CT. Thus, EdTx induced $CD4^+$ T cells secreting both IFN-γ and Th2-type cytokines. Further, EdTx as an adjuvant promoted only modest levels of OVA-specific IgE ($\log_2$ titers = 3) when compared with those seen after nasal immunization with CT (i.e., $\log_2$ titers = 8). Although it has been suggested that ATRs may not be expressed at the apical membrane of epithelial cells (50), there is no information to date on the relative expression of ATRs on immune cells and potential cellular targets of nasally administered EdTx. We have shown here that PA alone or as a component of EdTx does not target olfactory tissues and do not induce IL-1-specific mRNA in ON/E. It is also important to note that EdTx promotes a similar profile of serum Ab responses than CTA1-DD which targets B cells (31).

The mechanisms underlying the induction of mucosal immunity and S-IgA Ab responses by bacterial toxins remain only partially understood. Studies over the past two decades have shown a role for CT-induced cytokines on its mucosal adjuvanticity. Thus, CT was shown to induce both IL-6 and IL-1 secretion by epithelial cells and APCs (44, 58–60). Both IL-1 and IL-6 were later shown to be adjuvants for systemic immunity to nasally coadministered protein vaccines (38, 61) and IL-1 was also able to promote mucosal IgA Ab responses (61). Other factors thought to contribute to the adjuvanticity of CT include its ability to up-regulate the expression of MHC (44) and costimulatory molecules (45, 46, 62).

Table II. *Ag-specific $CD4^+$ T cell cytokine responses induced by nasal EdTx as an adjuvant*[a]

Immunization	In vitro Stimulation	Cytokines (pg/ml)			
		IFN-γ	IL-5	IL-6	IL-13
OVA only	None	156 ± 30	BD	36 ± 1	20 ± 2
	OVA	1320 ± 49*	41 ± 1*	175 ± 10*	36 ± 6
	PA	189 ± 10	BD	31 ± 1	20 ± 0
OVA plus EdTx	None	267 ± 37	BD	31 ± 1	20 ± 0
	OVA	9666 ± 1524*	418 ± 85*	386 ± 16*	188 ± 29*
	PA	16550 ± 2557*	1340 ± 160*	192 ± 28*	406 ± 78*

[a] Spleen $CD4^+$ T cells were isolated 21 days after the initial immunization and restimulated in vitro with OVA (1 mg/ml) or PA (20 μg/ml). Culture supernatants were collected after 5 days and cytokines evaluated by ELISA. The results are expressed as the mean ± 1 SE and are representative of four separate experiments. The same profile of responses was seen with $CD4^+$ T cells isolated from corresponding cervical lymph nodes. BD, Below detection levels; *, $p < 0.05$

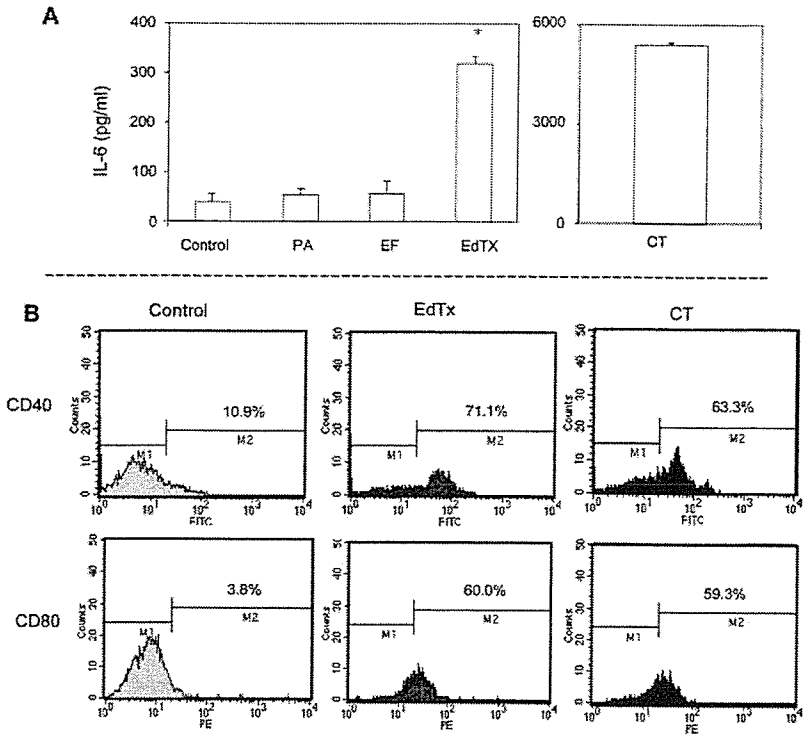

FIGURE 4. Effects of EdTx on cytokine secretion and costimulatory molecule expression by Mϕ. The J774 Mϕ were cultured for 48 h in the presence of PA (5 μg/ml), EF (5 μg/ml), EdTx (5 μg/ml PA + 5 μg/ml EF), or CT (1 μg/ml). *A*, Cytokine secretion was analyzed in culture supernatants, and results were expressed as mean ± 1 SD of four separate experiments (*, $p < 0.05$). *B*, Cells were analyzed by flow cytometry for expression CD40 and CD86. Results are representative of four separate experiments.

We have shown that EdTx stimulates IL-6 secretion by Mϕ cultures and enhances the expression of costimulatory molecules. We should stress that IL-6 levels induced by EdTx were ~10-fold lower than those seen in Mϕ cultures stimulated with the same dose of CT. The lower stimulatory effect of EdTx for IL-6 secretion was further confirmed in vivo where nasal delivery of CT but not EdTx induced IL-6 secretion in nasal washes. It is unlikely that the reduced ability of EdTx to induce IL-6 (and IL-1) could alone explain the polarized Ag-specific mucosal IgA Abs responses when compared with those generally induced by CT (34, 46, 63) or LT as adjuvants (34, 46, 54, 56). The role of the adenylate cyclase activity for the adjuvanticity remains to be elucidated. In this regard, the EF used in our studies contains a S447N mutation that could account for its recently reported 20-fold lower ability to

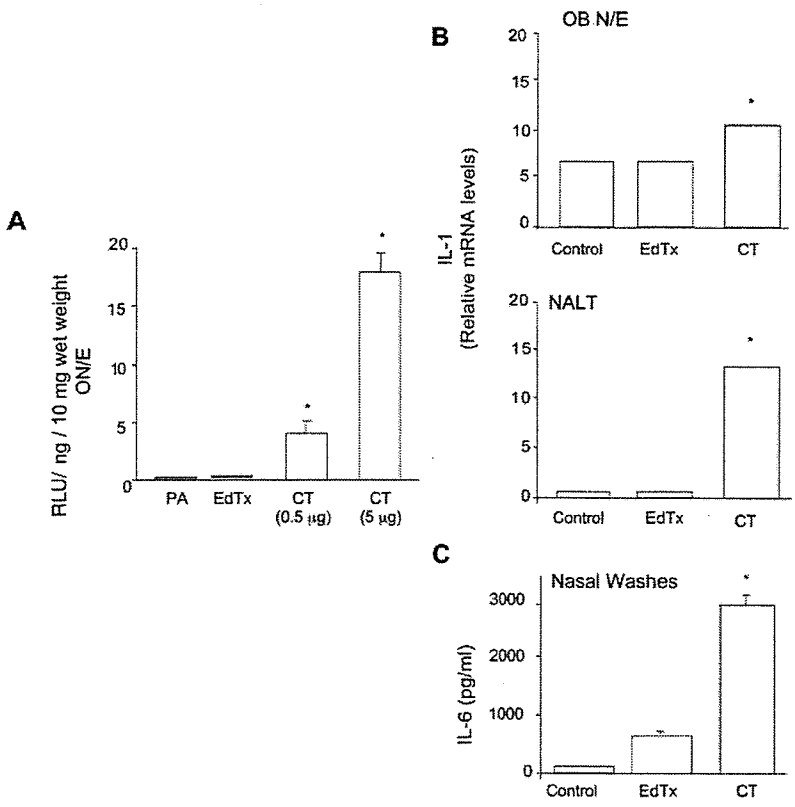

FIGURE 5. *A*, Tracking uptake into olfactory and CNS tissues. Groups of mice were given acridinium-labeled PA (5 μg), EdTx (5 μg of PA plus 5 μg of EF), or CT (0.5 or 5 μg) by the nasal route. *A*, Twenty-four hours later, mice were sacrificed and the ON/E and OBs were collected, homogenized, and tested for light activity as described in *Materials and Methods*. Results are expressed as mean RLU per nanogram of individual tissues ± 1 SD and are from two separate experiments with three mice per group (*, $p < 0.05$). *B*, IL-1 mRNA analysis by real-time RT-PCR. Results are expressed as mean relative mRNA levels from triplicate assays performed with pooled tissues (three mice per group) and are representative of three separate experiments (*, $p < 0.05$). *C*, Analysis of IL- 6 levels in nasal washes by ELISA. Results are expressed as picograms per milliliter ± 1 SD of IL-6 levels in individual nasal washes and are from two experiments with three mice per group. *, $p < 0.05$ when compared with controls given PBS.

induce cAMP when compared with recombinant native EF protein (33). Several mutants of both CT and LT-I, which are devoid of ADP-ribosyl transferase activity, were shown to retain their mucosal adjuvant activity and the ability to promote high mucosal IgA Ab responses. In another system, the mucosal adjuvant activity of CTA1-DD was reported to require both effective B cell targeting and the ADP ribosyl transferase activity (57). Thus, further studies are warranted to establish the mechanisms of mucosal adjuvanticity of EdTx.

Enterotoxin adjuvants are also potent immunogens which induce elevated immune responses to their binding subunits (41, 43). A major finding of this study resides in the fact that EdTx is a potent immunogen and that the presence of EF increased anti-PA responses above levels achieved after administration of PA alone. We have previously reported that high levels of PA-specific Abs could be detected in mouse plasma following nasal immunization with PA doses of up to 25 μg when CT was used as adjuvant (35). The same studies showed that 40 μg of PA/dose were needed to promote PA-specific mucosal IgA Abs. The results summarized here indicated that ATR targeting with much lower doses of PA (i.e., 5 μg) and EF allows the induction of PA-specific S-IgA Abs. Interestingly, increasing the dose of PA given with EF to 40 μg did not increase the levels of PA-specific mucosal IgA Abs, suggesting that codelivery of EF achieved optimal S-IgA Ab responses with low nasal dose of PA. Although, nasal immunization with CT or LT-I as adjuvant primarily promotes IgA Ab responses in the respiratory and genitourinary tracts, low but significant responses are consistently seen in the gastrointestinal tract. PA was previously reported to deliver a functionally active CT-A subunit into mammalian cells using an LF^{1-254}-CT-A fusion protein (64). Therefore, it will be interesting to examine whether the ATR-mediated cellular targeting, the adenylate cyclase, and possibly other activities of EF govern the polarized PA-specific mucosal IgA Ab responses induced by EdTx as adjuvant.

In summary, we have shown that ATR targeting of an adenylate cyclase subunit provides an effective strategy for enhancing the immune response to nasal vaccines. The EdTx as nasal adjuvant does not target the olfactory or other CNS tissues and thus could represent a safer alternative to ganglioside-binding adjuvants. In addition, EdTx very efficiently promoted anti-PA Ab responses both in saliva and in plasma and this could have important implications for improving the efficacy of current PA-based anthrax vaccines.

Disclosures

The authors have no financial conflict of interest.

References

1. Mock, M., and A. Fouet. 2001. Anthrax. *Annu. Rev. Microbiol.* 55: 647–644.
2. Collier, R. J., and J. A. Young. 2003. Anthrax toxin. *Annu. Rev. Cell Dev. Biol.* 19: 45–70.
3. Moayeri, M., and S. H. Leppla. 2004. The roles of anthrax toxin in pathogenesis. *Curr. Opin. Microbiol.* 7: 19–24.
4. Bradley, K. A., J. Mogridge, M. Mourez, R. J. Collier, and J. A. Young. 2001. Identification of the cellular receptor for anthrax toxin. *Nature* 414: 225–229.
5. Scobie, H. M., G. J. Rainey, K. A. Bradley, and J. A. Young. 2003. Human capillary morphogenesis protein 2 functions as an anthrax toxin receptor. *Proc. Natl. Acad. Sci. USA* 100: 5170–5174.
6. Leppla, S. H. 1982. Anthrax toxin edema factor: a bacterial adenylate cyclase that increases cyclic AMP concentrations of eukaryotic cells. *Proc. Natl. Acad. Sci. USA* 79: 3162–3166.
7. Guo, Q., Y. Shen, N. L. Zhukovskaya, J. Florian, and W. J. Tang. 2004. Structural and kinetic analyses of the interaction of anthrax adenylyl cyclase toxin with reaction products cAMP and pyrophosphate. *J. Biol. Chem.* 279: 29427–29435.
8. Shen, Y., N. L. Zhukovskaya, Q. Guo, J. Florian, and W. J. Tang. 2005. Calcium-independent calmodulin binding and two-metal-ion catalytic mechanism of anthrax edema factor. *EMBO J.* 24: 929–941.
9. Singh, Y., S. H. Leppla, R. Bhatnagar, and A. M. Friedlander. 1989. Internalization and processing of *Bacillus anthracis* lethal toxin by toxin-sensitive and -resistant cells. *J. Biol. Chem.* 264: 11099–11102.
10. Friedlander, A. M., R. Bhatnagar, S. H. Leppla, L. Johnson, and Y. Singh. 1993. Characterization of macrophage sensitivity and resistance to anthrax lethal toxin. *Infect. Immun.* 61: 245–252.
11. Hanna, P. C., D. Acosta, and R. J. Collier. 1993. On the role of macrophages in anthrax. *Proc. Natl. Acad. Sci. USA* 90: 10198–10201.
12. Agrawal, A., J. Lingappa, S. H. Leppla, S. Agrawal, A. Jabbar, C. Quinn, and B. Pulendran. 2003. Impairment of dendritic cells and adaptive immunity by anthrax lethal toxin. *Nature* 424: 329–334.
13. Ballard, J. D., R. J. Collier, and M. N. Starnbach. 1996. Anthrax toxin-mediated delivery of a cytotoxic T-cell epitope in vivo. *Proc. Natl. Acad. Sci. USA* 93: 12531–12534.
14. Goletz, T. J., K. R. Klimpel, N. Arora, S. H. Leppla, J. M. Keith, and J. A. Berzofsky. 1997. Targeting HIV proteins to the major histocompatibility complex class I processing pathway with a novel gp120-anthrax toxin fusion protein. *Proc. Natl. Acad. Sci. USA* 94: 12059–12064.
15. Brossier, F., M. Weber-Levy, M. Mock, and J. C. Sirard. 2000. Protective antigen-mediated antibody response against a heterologous protein produced in vivo by *Bacillus anthracis*. *Infect. Immun.* 68: 5731–5734.
16. Lu, Y., R. Friedman, N. Kushner, A. Doling, L. Thomas, N. Touzjian, M. Starnbach, and J. Lieberman. 2000. Genetically modified anthrax lethal toxin safely delivers whole HIV protein antigens into the cytosol to induce T cell immunity. *Proc. Natl. Acad. Sci. USA* 97: 8027–8032.
17. Kushner, N., D. Zhang, N. Touzjian, M. Essex, J. Lieberman, and Y. Lu. 2003. A fragment of anthrax lethal factor delivers proteins to the cytosol without requiring protective antigen. *Proc. Natl. Acad. Sci. USA* 100: 6652–6657.
18. Price, B. M., A. L. Liner, S. Park, S. H. Leppla, A. Mateczun, and D. R. Galloway. 2001. Protection against anthrax lethal toxin challenge by genetic immunization with a plasmid encoding the lethal factor protein. *Infect. Immun.* 69: 4509–4515.
19. Kumar, P., N. Ahuja, and R. Bhatnagar. 2002. Anthrax edema toxin requires influx of calcium for inducing cyclic AMP toxicity in target cells. *Infect. Immun.* 70: 4997–5007.
20. Paccani, S. R., F. Tonello, R. Ghittoni, M. Natale, L. Muraro, M. M. D'Elios, W. J. Tang, C. Montecucco, and C. T. Baldari. 2005. Anthrax toxins suppress T lymphocyte activation by disrupting antigen receptor signaling. *J. Exp. Med.* 201: 325–331.
21. Spangler, B. D. 1992. Structure and function of cholera toxin and the related *Escherichia coli* heat-labile enterotoxin. *Microbiol. Rev.* 56: 622–647.
22. Gill, D. M. 1976. The arrangement of subunits in cholera toxin. *Biochemistry* 15: 1242–1248.
23. Gill, D. M., J. D. Clements, D. C. Robertson, and R. A. Finkelstein. 1981. Subunit number and arrangement in *Escherichia coli* heat-labile enterotoxin. *Infect. Immun.* 33: 677–682.
24. Heyningen, S. V. 1974. Cholera toxin: interaction of subunits with ganglioside GM1. *Science* 183: 656–657.
25. Holmgren, J., M. Lindblad, P. Fredman, L. Svennerholm, and H. Myrvold. 1985. Comparison of receptors for cholera and *Escherichia coli* enterotoxins in human intestine. *Gastroenterology* 89: 27–35.
26. Griffiths, S. L., R. A. Finkelstein, and D. R. Critchley. 1986. Characterization of the receptor for cholera toxin and *Escherichia coli* heat-labile toxin in rabbit intestinal brush borders. *Biochem. J.* 238: 313–322.
27. Fukuta, S., J. L. Magnani, E. M. Twiddy, R. K. Holmes, and V. Ginsburg. 1988. Comparison of the carbohydrate-binding specificities of cholera toxin and *Escherichia coli* heat-labile enterotoxins LTh-I, LT-IIa, and LT-IIb. *Infect. Immun.* 56: 1748–1753.
28. Couch, R. B. 2004. Nasal vaccination, *Escherichia coli* enterotoxin, and Bell's palsy. *N. Engl. J. Med.* 350: 860–861.
29. Mutsch, M., W. Zhou, P. Rhodes, M. Bopp, R. T. Chen, T. Linder, C. Spyr, and R. Steffen. 2004. Use of the inactivated intranasal influenza vaccine and the risk of Bell's palsy in Switzerland. *N. Engl. J. Med.* 350: 896–903.
30. van Ginkel, F. W., R. J. Jackson, Y. Yuki, and J. R. McGhee. 2000. Cutting edge: the mucosal adjuvant cholera toxin redirects vaccine proteins into olfactory tissues. *J. Immunol.* 165: 4778–4782.
31. Eriksson, A. M., K. M. Schon, and N. Y. Lycke. 2004. The cholera toxin-derived CTA1-DD vaccine adjuvant administered intranasally does not cause inflammation or accumulate in the nervous tissues. *J. Immunol.* 173: 3310–3319.
32. Ramirez, D. M., S. H. Leppla, R. Schneerson, and J. Shiloach. 2002. Production, recovery and immunogenicity of the protective antigen from a recombinant strain of *Bacillus anthracis*. *J. Ind. Microbiol. Biotechnol.* 28: 232–238.
33. Cooksey, B. A., G. C. Sampey, J. L. Pierre, X. Zhang, J. D. Karwoski, G. H. Choi, and M. W. Laird. 2004. Production of biologically active *Bacillus anthracis* edema factor in *Escherichia coli*. *Biotechnol. Prog.* 20: 1651–1659.
34. Boyaka, P. N., M. Ohmura, K. Fujihashi, T. Koga, M. Yamamoto, M. N. Kweon, Y. Takeda, R. J. Jackson, H. Kiyono, Y. Yuki, and J. R. McGhee. 2003. Chimeras of labile toxin one and cholera toxin retain mucosal adjuvanticity and direct Th cell subsets via their B subunit. *J. Immunol.* 170: 454–462.
35. Boyaka, P. N., A. Tafaro, R. Fischer, S. H. Leppla, K. Fujihashi, and J. R. McGhee. 2003. Effective mucosal immunity to anthrax: neutralizing antibodies and Th cell responses following nasal immunization with protective antigen. *J. Immunol.* 170: 5636–5643.
36. Mosmann, T. 1983. Rapid colorimetric assay for cellular growth and survival: application to proliferation and cytotoxicity assays. *J. Immunol. Methods* 65: 55–63.
37. Lillard, J. W., Jr., U. P. Singh, P. N. Boyaka, S. Singh, D. D. Taub, and J. R. McGhee. 2003. MIP-1α and MIP-1β differentially mediate mucosal and systemic adaptive immunity. *Blood* 101: 807–814.

38. Boyaka, P. N., M. Marinaro, R. J. Jackson, S. Menon, H. Kiyono, E. Jirillo, and J. R. McGhee. 1999. IL-12 is an effective adjuvant for induction of mucosal immunity. *J. Immunol.* 162: 122–128.
39. Livak, K. J., and T. D. Schmittgen. 2001. Analysis of relative gene expression data using real-time quantitative PCR and the $2(-\Delta\Delta C_T)$ method. *Methods* 25: 402–408.
40. Elson, C. O., and W. Ealding. 1984. Cholera toxin feeding did not induce oral tolerance in mice and abrogated oral tolerance to an unrelated protein antigen. *J. Immunol.* 133: 2892–2897.
41. Elson, C. O., and W. Ealding. 1984. Generalized systemic and mucosal immunity in mice after mucosal stimulation with cholera toxin. *J. Immunol.* 132: 2736–2741.
42. Clements, J. D., N. M. Hartzog, and F. L. Lyon. 1988. Adjuvant activity of *Escherichia coli* heat-labile enterotoxin and effect on the induction of oral tolerance in mice to unrelated protein antigens. *Vaccine* 6: 269–277.
43. Elson, C. O., and M. T. Dertzbaugh. 1999. Mucosal adjuvants. In *Mucosal Immunology*. P. L. Ogra, J. Mestecky, M. E. Lamm, W. Strober, J. Bienenstock, and J. R. McGhee, eds. Academic Press, San Diego, pp. 817–838.
44. Bromander, A. K., M. Kjerrulf, J. Holmgren, and N. Lycke. 1993. Cholera toxin enhances alloantigen presentation by cultured intestinal epithelial cells. *Scand. J. Immunol.* 37: 452–458.
45. Cong, Y., C. T. Weaver, and C. O. Elson. 1997. The mucosal adjuvanticity of cholera toxin involves enhancement of costimulatory activity by selective upregulation of B7.2 expression. *J. Immunol.* 159: 5301–5308.
46. Yamamoto, M., H. Kiyono, M. N. Kweon, S. Yamamoto, K. Fujihashi, H. Kurazono, K. Imaoka, H. Bluethmann, I. Takahashi, Y. Takeda, et al. 2000. Enterotoxin adjuvants have direct effects on T cells and antigen-presenting cells that result in either interleukin-4-dependent or -independent immune responses. *J. Infect. Dis.* 182: 180–190.
47. Agren, L. C., L. Ekman, B. Lowenadler, and N. Y. Lycke. 1997. Genetically engineered nontoxic vaccine adjuvant that combines B cell targeting with immunomodulation by cholera toxin A1 subunit. *J. Immunol.* 158: 3936–3946.
48. Agren, L., E. Sverremark, L. Ekman, K. Schon, B. Lowenadler, C. Fernandez, and N. Lycke. 2000. The ADP-ribosylating CTA1-DD adjuvant enhances T cell-dependent and independent responses by direct action on B cells involving anti-apoptotic Bcl-2- and germinal center-promoting effects. *J. Immunol.* 164: 6276–6286.
49. Bonuccelli, G., F. Sotgia, P. G. Frank, T. M. Williams, C. J. de Almeida, H. B. Tanowitz, P. E. Scherer, K. A. Hotchkiss, B. I. Terman, B. Rollman, et al. 2005. Anthrax toxin receptor (ATR/TEM8) is highly expressed in epithelial cells lining the toxin's three sites of entry (lung, skin, and intestine). *Am. J. Physiol.* 288: C1402–C1410.
50. Beauregard, K. E., S. Wimer-Mackin, R. J. Collier, and W. I. Lencer. 1999. Anthrax toxin entry into polarized epithelial cells. *Infect. Immun.* 67: 3026–3030.
51. Doling, A. M., J. D. Ballard, H. Shen, K. M. Krishna, R. Ahmed, R. J. Collier, and M. N. Starnbach. 1999. Cytotoxic T-lymphocyte epitopes fused to anthrax toxin induce protective antiviral immunity. *Infect. Immun.* 67: 3290–3296.
52. Marinaro, M., H. F. Staats, T. Hiroi, R. J. Jackson, M. Coste, P. N. Boyaka, N. Okahashi, M. Yamamoto, H. Kiyono, H. Bluethmann, et al. 1995. Mucosal adjuvant effect of cholera toxin in mice results from induction of T helper 2 (Th2) cells and IL-4. *J. Immunol.* 155: 4621–4629.
53. Vajdy, M., M. H. Kosco-Vilbois, M. Kopf, G. Kohler, and N. Lycke. 1995. Impaired mucosal immune responses in interleukin 4-targeted mice. *J. Exp. Med.* 181: 41–53.
54. Takahashi, I., M. Marinaro, H. Kiyono, R. J. Jackson, I. Nakagawa, K. Fujihashi, S. Hamada, J. D. Clements, K. L. Bost, and J. R. McGhee. 1996. Mechanisms for mucosal immunogenicity and adjuvancy of *Escherichia coli* labile enterotoxin. *J. Infect. Dis.* 173: 627–635.
55. Okahashi, N., M. Yamamoto, J. L. Vancott, S. N. Chatfield, M. Roberts, H. Bluethmann, T. Hiroi, H. Kiyono, and J. R. McGhee. 1996. Oral immunization of interleukin-4 (IL-4) knockout mice with a recombinant *Salmonella* strain or cholera toxin reveals that $CD4^+$ Th2 cells producing IL-6 and IL-10 are associated with mucosal immunoglobulin A responses. *Infect. Immun.* 64: 1516–1525.
56. Kweon, M. N., M. Yamamoto, F. Watanabe, S. Tamura, F. W. Van Ginkel, A. Miyauchi, H. Takagi, Y. Takeda, T. Hamabata, K. Fujihashi, et al. 2002. A nontoxic chimeric enterotoxin adjuvant induces protective immunity in both mucosal and systemic compartments with reduced IgE antibodies. *J. Infect. Dis.* 186: 1261–1269.
57. Agren, L. C., L. Ekman, B. Lowenadler, J. G. Nedrud, and N. Y. Lycke. 1999. Adjuvanticity of the cholera toxin A1-based gene fusion protein, CTA1-DD, is critically dependent on the ADP-ribosyltransferase and Ig-binding activity. *J. Immunol.* 162: 2432–2440.
58. Lycke, N., A. K. Bromander, L. Ekman, U. Karlsson, and J. Holmgren. 1989. Cellular basis of immunomodulation by cholera toxin in vitro with possible association to the adjuvant function in vivo. *J. Immunol.* 142: 20–27.
59. Bromander, A., J. Holmgren, and N. Lycke. 1991. Cholera toxin stimulates IL-1 production and enhances antigen presentation by macrophages in vitro. *J. Immunol.* 146: 2908–2914.
60. McGee, D. W., C. O. Elson, and J. R. McGhee. 1993. Enhancing effect of cholera toxin on interleukin-6 secretion by IEC-6 intestinal epithelial cells: mode of action and augmenting effect of inflammatory cytokines. *Infect. Immun.* 61: 4637–4644.
61. Staats, H. F., and F. A. Ennis, Jr. 1999. IL-1 is an effective adjuvant for mucosal and systemic immune responses when coadministered with protein immunogens. *J. Immunol.* 162: 6141–6147.
62. Gagliardi, M. C., F. Sallusto, M. Marinaro, S. Vendetti, A. Riccomi, and M. T. De Magistris. 2002. Effects of the adjuvant cholera toxin on dendritic cells: stimulatory and inhibitory signals that result in the amplification of immune responses. *Int. J. Med. Microbiol.* 291: 571–575.
63. Yamamoto, S., H. Kiyono, M. Yamamoto, K. Imaoka, K. Fujihashi, F. W. Van Ginkel, M. Noda, Y. Takeda, and J. R. McGhee. 1997. A nontoxic mutant of cholera toxin elicits Th2-type responses for enhanced mucosal immunity. *Proc. Natl. Acad. Sci. USA* 94: 5267–5272.
64. Sharma, M., H. Khanna, N. Arora, and Y. Singh. 2000. Anthrax toxin-mediated delivery of cholera toxin-A subunit into the cytosol of mammalian cells. *Biotechnol. Appl. Biochem.* 32(Pt. 1): 69–72.

A Second Generation of Double Mutant Cholera Toxin Adjuvants: Enhanced Immunity without Intracellular Trafficking[1]

Yukari Hagiwara,*† Yuki I. Kawamura,‡ Kosuke Kataoka,* Bibi Rahima,* Raymond J. Jackson,* Katsuhiro Komase,† Taeko Dohi,‡ Prosper N. Boyaka,* Yoshifumi Takeda,§ Hiroshi Kiyono,*¶ Jerry R. McGhee,* and Kohtaro Fujihashi[2]*

Nasal application of native cholera toxin (nCT) as a mucosal adjuvant has potential toxicity for the CNS through binding to GM1 gangliosides in the olfactory nerves. Although mutants of cholera toxin (mCTs) have been developed that show mucosal adjuvant activity without toxicity, it still remains unclear whether these mCTs will induce CNS damage. To help overcome these concerns, in this study we created new double mutant CTs (dmCTs) that have two amino acid substitutions in the ADP-ribosyltransferase active center (E112K) and COOH-terminal KDEL (E112K/KDEV or E112K/KDGL). Confocal microscopic analysis showed that intracellular localization of dmCTs differed from that of mCTs and nCTs in intestinal epithelial T84 cells. Furthermore, both dmCTs exhibited very low toxicity in the Y1 cell assay and mouse ileal loop tests. When mucosal adjuvanticity was examined, both dmCTs induced enhanced OVA-specific immune responses in both mucosal and systemic lymphoid tissues. Interestingly, although both dmCT E112K/KDEV and dmCT E112K/KDGL showed high Th2-type and significant Th1-type cytokine responses by OVA-specific CD4$^+$ T cells, dmCT E112K/KDEV exhibited significantly lower Th1-type cytokine responses than did nCT and dmCT E112K/KDGL. These results show that newly developed dmCTs retain strong biological adjuvant activity without CNS toxicity. *The Journal of Immunology,* **2006, 177: 3045–3054.**

An important aspect of immune responses at mucosal surfaces is the production of polymeric IgA Abs, as well as their transport across the epithelium and release as secretory IgA (S-IgA).[3] Because this S-IgA Ab response represents the first major line of defense against invasion by viral and bacterial pathogens (1), recent efforts have been focused on the development of vaccines that are capable of inducing effective immune responses in mucosal tissues. However, most protein Ags are rather weak immunogens when given by a mucosal route. If the full potential of the new generation of mucosal vaccines is to be realized, effective and reliable mucosal adjuvants must be developed.

Our recent study (2) showed that nasal vaccines for nasopharyngeal-associated lymphoreticular tissue (NALT)-based mucosal immunity could make a significant contribution to protecting the elderly. Furthermore, these nasal and oral vaccines would be easier to administer than parenteral ones. Mucosal vaccines would also carry less risk of transmitting infections like hepatitis B and HIV, which are still associated with the use of injectable vaccines in several parts of the world. Despite these many attractive features, it has often proved difficult in practice to stimulate strong mucosal S-IgA Ab responses with subsequent protection by the use of mucosal administration of vaccines, and the results to date for mucosal vaccinations using soluble protein Ags have been, with a few notable exceptions, rather disappointing (3).

Native cholera toxin (nCT) produced by *Vibrio cholerae* is structurally similar to the native heat-labile enterotoxin (nLT) of enterotoxigenic *Escherichia coli*. Both toxins act as adjuvants for the enhancement of mucosal and systemic Ab responses to coadministered protein Ags given by either oral or nasal routes (4–7) and, consequently, are the most widely used experimental mucosal adjuvants in animal models. Furthermore, both act as mucosal adjuvants by inducing CD4$^+$ Th2 cells secreting IL-4, IL-5, IL-6, and IL-10, which provide help for Ag-specific S-IgA as well as plasma IgG1, IgA, and IgE Ab responses (8, 9). Although they are potent mucosal adjuvants, both nCT and nLT are also toxic and, thus, are not suitable for use with mucosal vaccines in humans. Therefore, a number of nontoxic mutant derivatives of cholera toxin (CT) or heat-labile enterotoxin (LT) have been constructed.

Our own group has contributed to the efforts of constructing nontoxic mutant derivatives; we generated two mutant CTs (mCTs), mCT S61F and mCT E112K, by substituting a single amino acid in the ADP-ribosyltransferase active center of the A

*Departments of Pediatric Dentistry and Microbiology, Immunobiology Vaccine Center, University of Alabama at Birmingham, Birmingham, AL 35294; †Research Center for Biologicals, Kitasato Institute, Saitama, Japan; ‡Department of Gastroenterology, Research Institute, International Medical Center of Japan, Tokyo, Japan; §Cine-Science Laboratory Co. Ltd., Tokyo, Japan; and ¶Division of Mucosal Immunology, Department of Microbiology and Immunology, Institute of Medical Science, University of Tokyo, Tokyo, Japan

Received for publication September 27, 2005. Accepted for publication June 10, 2006.

The costs of publication of this article were defrayed in part by the payment of page charges. This article must therefore be hereby marked *advertisement* in accordance with 18 U.S.C. Section 1734 solely to indicate this fact.

[1] This research was supported by National Institutes of Health Grants DC 04976, DE 12242, AI 18958, and AI 43197 and Grants-in-Aid from the Ministry of Health and Labor, Japan, the Ministry of Education, Science and Sports, Japan, and CREST of Japan Science and Technology Corporation.

[2] Address correspondence and reprint requests to Dr. Kohtaro Fujihashi, Department of Pediatric Dentistry, Immunobiology Vaccine Center, University of Alabama at Birmingham, 761 Bevill Biomedical Research Building, 845 19th Street South, Birmingham, AL 35294-2170. E-mail address: kohtarof@uab.edu

[3] Abbreviations used in this paper: S-IgA, secretory IgA; AFC, Ab forming cell; CHO, Chinese hamster ovary; CLN, cervical lymph node; CT, cholera toxin; nCT, native CT; CT-A, A subunit of nCT; CT-B, B subunit of nCT; dmCT, double mutant CT; mCT, mutant CT; DD, dimer of an Ig binding element; ER, endoplasmic reticulum; LT, heat-labile enterotoxin; nLT, native LT; NALT, nasopharyngeal-associated lymphoreticular tissue; NP, nasal passage; OB, olfactory bulb; ON/E, olfactory nerves and epithelium; SMG, submandibular gland.

0022-1767/06/$02.00

subunit (10, 11). Although these originally created forms of mCT did not induce ADP-ribosylation and cAMP formation, they still served as mucosal adjuvants by inducing $CD4^+$ Th2 cells, thereby providing effective help for Ag-specific, mucosal S-IgA, as well as plasma IgG and IgA Ab responses.

It is clearly too dangerous to use an enterotoxin as an adjuvant for mucosal vaccines in humans. Our previous studies have shown that nasally administered nCT accumulates in the olfactory nerves and epithelium (ON/E) and olfactory bulbs (OBs) of mice after binding to GM1 gangliosides (12). Furthermore, nCT as a mucosal adjuvant redirects coadministered protein Ags into these neuronal tissues (12). This finding has provoked some concern about the potential role for ganglioside GM1-binding molecules that target neuronal tissues, including the CNS, in nasal immunization. Although deposition of nCT via the ON/E and OBs did not lead to obvious pathologic changes in brain tissue after nasal administration (13), it has been reported that a human vaccine containing inactivated influenza and nLT as an adjuvant resulted in a very high incidence of Bell's palsy (14, 15). These results strongly indicate that it is essential to develop a safer and more effective nasal adjuvant for human use.

Both nCT and nLT consist of a ring of five B subunits and a single A subunit that is cleaved into A1 and A2 chains. Previous studies showed that the carboxyl terminus of the A2 subunit of nCT contains the ER retention signal tetrapeptide KDEL (RDEL in LT). These results show that the toxin is transported via the vesicles from the plasma membrane to the Golgi compartment with subsequent separation of the A and B subunits of nCT (designated throughout as CT-A and CT-B, respectively). The CT-A subunit is redirected to the plasma membrane by retrograde transport via the ER, whereas the CT-B subunit persists in the Golgi compartment. The intracellular target of toxin is G_s, the stimulatory regulatory component of adenyl cyclase (16, 17). Thus, mutations in KDEL influence the movement of CT from the Golgi apparatus to the ER (18–21). It has previously been shown that mutation in K(R)DEL of both CT and LT delayed the time course of toxin-induced Cl^- secretion. Furthermore, consistent with a slower rate of signal transduction, KDEL mutants trafficked more slowly to the basolateral membrane than did nCT (18, 19).

However, a recent report indicated that mutant LT RDEL retained ADP-ribosyltransferase activity and induced morphological changes in Chinese hamster ovary (CHO) cell cultures (19). In contrast, mCT E112K has proven to be a safe and stable adjuvant (10, 11, 13, 22). The mCT E112K was constructed to be devoid of toxicity while retaining its adjuvant activity. Our previous studies showed that mCT E112K was effective in the murine system. Nasal immunization of OVA, the pneumococcal surface protein A of *Streptococcus pneumoniae*, or diphtheria toxoid plus mCT E112K elicited both Ag-specific IgA and IgG Ab responses in mucosal and systemic immune compartments (10, 11, 13). Although our recent studies showed that mCT E112K did not elicit any neuronal damage based upon nerve growth factor-β1 production in the CNS as well as Ag redirection (23, 24), these studies did not provide any direct information as to whether mCT E112K migrates into the CNS after nasal application. In this regard, we have developed double mutants of CT (dmCTs) by introducing a potent mutation in the ADP-ribosylation activity center and KDEL (E112K/KDEV or E112K/KDGL). Therefore, it is now essential for us to determine whether potentially less trafficking of these new dmCTs, when compared with mCT E112K, will occur in their distribution into the CNS. In this study, we have examined the mucosal adjuvanticity and toxicity of these two dmCTs for our continuing efforts to develop safe and effective nasal adjuvants for mucosal vaccines.

Materials and Methods

Preparation of recombinant mCTs

The plasmids containing nCT or mCT E112K genes were constructed as described previously (10). These plasmids were cloned into pUC119 of a 3.1-kb *Eco*RI/*Pst*I DNA fragment including nCT or mCT E112K genes (10). The KDGL and KDEV mutants were constructed by site-directed mutagenesis in which amino acid substitutions were introduced on a plasmid of nCT using PCR. The following oligonucleotides were used to create genes encoding the mutant toxins KDEV and KDGL: 5′-TAA GGA TGA AGT ATG ATT AAA TTA A-3′ and 5′-TAG AAT TAA GGA TGG ATT ATG ATT A-3′ (mutant codons underlined). To construct dmCT E112K/KDEV and E112K/KDGL, the *Bsp*EI/*Hin*cII fragments including KDEV or KDGL mutations were ligated to a plasmid of mCT E112K. After the DNA sequences were confirmed, pUC119 harboring the mutated CT genes at the *Eco*RI/*Pst*I site were transformed into *E. coli* DH5-α. The *E. coli* strains containing the plasmids for the dmCT genes were grown in Luria-Bertani medium (10 g of NaCl, 10 g of tryptone, and 5 g of yeast extract per liter) with 100 μg/ml ampicillin, and dmCTs were purified according to the method described previously (25). Briefly, the bacteria were harvested and lysed with a sonicator (Insonator 201M; Kubota). The crude lysate was then applied to an immobilized D-galactose column (Pierce) and eluted with galactose. The purified recombinant dmCTs contained <0.05 endotoxin U/μg protein.

Intracellular tracking

Human intestinal epithelial T84 cells were incubated with 10 μg/ml Alexa Fluor 488-conjugated nCT, mCT E112K, dmCT E112K/KDEV, or dmCT E112K/EDGL. To identify their intracellular destination, we used boron dipyrromethane Texas Red ceramide (Invitrogen Life Technologies) as a marker for the Golgi apparatus (26) and ER-Tracker (Invitrogen Life Technologies) Blue-White *p*-xylene-bis-pyridinium bromide as a marker for the ER (27). Boron dipyromethane Texas Red-ceramide was added to individual cultures at a concentration of 5 μM for 10 min before termination of the cultures. Cells were washed once before being further cultured in medium containing 2 μM ER-Tracker for 30 min. After incubation, cells were washed three times with PBS and then fixed with 3.7% formaldehyde in PBS for 10 min at room temperature. After fixation, a Leica TCS SP2-AOBS model confocal microscope or a LMS510 model confocal microscope (Zeiss) was used to visualize the cells. The merged color (yellow) area of each Golgi or ER staining image was picked up using Adobe Photoshop software and converted into a black and white picture. The black area in this black and white picture is based upon the original yellow color and was measured using ImageJ (National Institutes of Health). The condition for picking up the yellow area was saved and applied to all pictures. A monolayer of T84 cells covered most of the dish surface; however, for accuracy, we measured the total pixel area covered with cells in the identical picture using ImageJ software. Thus, each picture covers 12.96 mm^2 of culture surface, which is equal to 262144 pixels. The results were shown as the percentage of yellow color area pixels per the total area pixels covered with cells.

Bioassay and toxicity analysis

We next studied the ability of newly created dmCTs and nCT (List Biological Laboratories) to induce toxic effects on cultured mouse Y-1 adrenal tumor cells, following a previously developed procedure (28). Briefly, serial dilutions of dmCT E112K/KDEV, dmCT E112K/KDGL, mCT E112K, or nCT were added to cultures of Y-1 cells at a density of 5×10^4 cells/well in 0.1 ml of F-10 medium (Invitrogen Life Technologies) containing 15% horse serum and 2.5% FCS and incubated at 37°C with 5% CO_2 for 24 h. Light microscopy was then used to examine cells for morphological changes such as the common "rounding" of cells. The toxin concentration required to initiate the rounding of Y-1 cells was determined. For the cAMP assay, 1.5×10^4 CHO cells in F-10 medium containing 1% FCS were cultured with 100 ng/ml dmCT E112K/KDEV, dmCT E112K/KDGL, mCT E112K, or nCT at 37°C with 5% CO_2 for 18 h. Intracellular cAMP measurement was done with an enzyme immunoassay kit (Amersham Biosciences). The protein amount for some samples was determined with a Coomassie protein assay reagent (Pierce), and the levels of cAMP were expressed as picomoles of cAMP per milligram of protein (10). The mouse ileal loop test was conducted essentially as described previously (29, 30). Briefly, the jejenum was ligated with a piece of cotton thread at a distance of ~3 cm from the pylorus. Immediately after ligation, each loop was injected with 0.1 ml of toxin or PBS (as a control). After 3 h, each loop was hung on a fixed clip and stretched by placing another clip weighing 2 g on the other end of the loop. Then, the length and weight of each loop were

measured. The weight/length ratio (mg/cm) was used to express the intensity of the reaction.

Mice

C57BL/6 mice were obtained from the Frederick Cancer Research Facility (National Cancer Institute, Frederick, MD) as well as Japan SLC at 8–12 wk of age. Upon arrival, all mice were immediately transferred to microisolators, maintained in horizontal laminar flow cabinets, and provided sterile food and water ad libitum. The health of the mice was tested semiannually, and all mice used in experiments were determined to be free of bacterial and viral pathogens.

CNS trafficking

We investigated the distribution of acridinium-labeled toxins in the ON/E and OBs after nasal immunization. In these experiments, we used acridinium-labeled toxins because acridinium is a chemiluminescent molecule that can be triggered with sodium hydroxide and hydrogen peroxide in a luminometer to emit light at 430 nm. Because of its high sensitivity, acridinium can be detected at levels as low as femtograms. nCT, mCT E112K, dmCT E112K/KDEV, and dmCT E112K/KDGL were labeled with acridinium as described elsewhere (31). Five or 0.5 μg of acridinium-labeled nCT, mCT E112K, dmCT E112K/KDEV, or dmCT E112K/KDGL was given nasally, and its distribution in CNS tissues was then checked after 24 h. In some experiments, mice were given nasal OVA plus 0.5 μg of acridinium-labeled nCT, mCT E112K, dmCT E112K/KDEV, or dmCT E112K/KDGL three times at weekly intervals. Seven days after the last immunization, residual amounts of enterotoxin in the CNS tissues were detected. For isolation of CNS tissues, we examined both ON/E and OBs as previously described (12). The levels of acridinium present were determined by triggering with sodium hydroxide and hydrogen peroxide in a luminometer emitting light at 430 nm. The CNS tissues of mice given nasal PBS were examined for their background levels of luminescence. These control values are subtracted from each experimental value.

Nasal immunization and sample collection

C57BL/6 mice were immunized three times at weekly intervals with a nasal dose of 100 μg of OVA (Fraction V; Sigma-Aldrich) and 0.5 μg of nCT, mCT E112K, dmCT E112K/KDEV, or dmCT E112K/KDGL in PBS (11, 22, 32). Plasma and mucosal secretions (nasal washes, saliva, and fecal extracts) were collected on day 21. Saliva was obtained from mice following i.p. injection of 100 μg of sterile pilocarpine hydrochloride (Sigma-Aldrich) (33). Fecal pellets (100 mg) were suspended in 1 ml of PBS containing 0.1% sodium azide and then extracted by vortexing for 5 min. The samples were spun at 10,000 × *g* for 5 min, and the supernatants were collected as fecal extracts (11, 22, 33). The nasal washes were obtained by injecting 1 ml of PBS containing 1% BSA on three occasions into the posterior opening of the nasopharynx with a hypodermic needle (34).

Ab assays

Ab titers in plasma and external secretions were determined by an ELISA (10, 11, 22, 35). Falcon microtest assay plates (BD Biosciences) were coated with an optimal concentration of OVA (100 μl of 1 mg/ml) in PBS overnight at 4°C. Two-fold serial dilutions of samples were added after blocking with PBS containing 1% BSA. To detect Ag-specific Ab levels, HRP-conjugated, goat anti-mouse μ, γ, or α H chain-specific Abs were used (Southern Biotechnology Associates). For IgG Ab subclass determinations, biotinylated mAbs specific for IgG1, IgG2a, IgG2b, and IgG3 (BD Pharmingen) and peroxidase-conjugated goat anti-biotin Ab were used. End point titers were expressed as the last dilution yielding an $OD_{414\ nm}$ of >0.1 U above negative control values after 15 min of incubation.

ELISA for OVA-specific IgE Ab responses

OVA-specific IgE Abs were determined by an ELISA (32). Plasma samples were collected 2 wk after the initial nasal immunization, because our previous studies showed that peak Ag-specific IgE Ab responses were seen at this time point, when mice were immunized with OVA and either nCT or mCT E112K as mucosal adjuvants (11). For detection of OVA-specific plasma IgE Ab levels, 96-well immunoplates (Nunc) were coated with rat anti-mouse IgE mAb (R35-72; BD Pharmingen) and incubated overnight at 4°C. After blocking with 3% BSA in PBS, serial dilutions of plasma samples were added and incubated overnight at 4°C. Following extensive washing, biotinylated OVA was added and the plates were incubated overnight at 4°C. Next, HRP-labeled goat anti-biotin Ab (Vector Laboratories) was added, and the color reaction was developed with 2, 2′-azino-bis(3-ethylbenzthiazoline-6-sulfonic acid) (Sigma). End point titers were expressed as the last dilution yielding an $OD_{414\ nm}$ of >0.1 U above negative control values after 15 min incubation.

Enumeration of Ab-forming cells (AFCs)

The spleen and cervical lymph nodes (CLNs) were removed aseptically, and single-cell suspensions were prepared as described elsewhere (11, 22, 32, 35). The submandibular glands (SMGs) and PBS-perfused lungs were removed aseptically and minced into small fragments. Mononuclear cells were isolated by a combination of an enzymatic dissociation procedure with collagenase type IV (0.5 mg/ml; Sigma-Aldrich) followed by discontinuous Percoll (Amersham Biosciences) gradient centrifugation (33). For isolation of mononuclear cells from NALT and nasal passages (NPs), a modified dissociation method was used based upon a previously described protocol (36–38). Individual NALTs were carefully removed using microsurgical tweezers under a stereoscopic microscope. Following removal of the NALT, the NP tissues were also removed from the nasal cavity. Cells from individual tissues were prepared by gently teasing them through sterile stainless steel screens, followed by enzymatic dissociation using collagenase type IV to obtain single-cell preparations (36–38). Mononuclear cells were purified by discontinuous Percoll gradients (Amersham Biosciences). Mononuclear cells in the interface between the 40 and 75% layers were removed, washed, and resuspended in RPMI 1640 (Mediatech) supplemented with HEPES buffer (15 mM), L-glutamine (2 mM), penicillin (100 U/ml), streptomycin (100 μg/ml), and 10% FCS (complete medium). Cells were then subjected to an OVA-specific ELISPOT assay to detect cells producing IgM, IgG, and IgA AFCs (11, 22, 32, 35). Ninety-six-well nitrocellulose plates (Millipore) were coated with 1 mg/ml OVA for analysis of anti-OVA specific AFCs (11, 32, 33).

OVA-specific T cell responses

$CD4^+$ T cells were purified by the magnetic-activated cell sorter system (Miltenyi Biotec) as described previously (11, 35). Briefly, cells from the spleen and CLNs were incubated in a nylon wool column (Polysciences) to remove B cells and macrophages. Enriched T cell fractions were then incubated with anti-mouse CD4 (GK 1.5) microbeads (Miltenyi Biotec) and passed through a magnetized column. The purified T cell fractions were >97% $CD4^+$ and >99% viable. Cells were resuspended in complete medium, and the purified $CD4^+$ T cells (4×10^6 cells/ml) were cultured with or without 1 mg/ml OVA in the presence of T cell-dependent, mitomycin C-treated splenic APCs. These APCs were derived from naive mice and were placed in 96-well or 24-well tissue culture plates (Corning Glass) for 5 days at 37°C in a moist atmosphere of 5% CO_2 in air. In some experiments, purified $CD4^+$ T cells from CLNs and spleen of naive mice were incubated with anti-CD3 mAb (10 μg/ml)- and anti-CD28 mAb (10 μg/ml)-coated wells for 2 days at 37°C in a moist atmosphere of 5% CO_2 in air.

Proliferation of $CD4^+$ T cells was assessed using a cell proliferation ELISA (Roche Diagnostic Systems). Briefly, 10 μmol of BrdU was added for the final 18 h of incubation. The plates were centrifuged at 300 × *g* for 10 min before drying. The plates were incubated with FixDenat solution (Roche) for 30 min at room temperature. Once the solution had been removed, the cells were labeled with a peroxidase-conjugated anti-BrdU mAb for 90 min at room temperature. The plates were washed with PBS-Tween 20 and then developed using a tetramethyl benzidine substrate solution. Incubations were terminated by addition of 1 M H_2SO_4. The absorbance of samples was measured by an ELISA reader at 450 nm. In some experiments, culture supernatants were harvested after 2 or 5 days of incubation and were then subjected to cytokine-specific ELISA.

Cytokine-specific ELISA

Levels of cytokines in culture supernatants were measured by ELISA. The details of the ELISA for IFN-γ, IL-2, IL-4, IL-5, IL-6, and IL-10 have been described previously (10, 39–41). For coating and detection, the following mAbs were used: for anti-IFN-γ, R4-6A2 and XMG1.2 mAbs; for anti-IL-2, JSE6-1A12 and JES-5H4 mAbs; for anti-IL-4, BVD4-1D11 and BVD6-24G2 mAbs; for anti-IL-5, TRFK-5 and TRFK-4 mAbs; for anti-IL-6, MP5-20F3 and MP5-32C11 mAbs; and for anti-IL-10, JES5-2A5 and JES5-16E3 mAbs. The levels of Ag-specific cytokine production were calculated by subtracting the results of control cultures (e.g., without OVA stimulation) from those of OVA-stimulated T cell cultures. This ELISA was capable of detecting 0.10 ng/ml IFN-γ, 30.5 pg/ml IL-2, 23.4 pg/ml IL-4, 6.1 pg/ml IL-5, 78.1 pg/ml IL-6, and 24.4 ng/ml IL-10.

Statistics

The data are expressed as the mean ± SEM. Each mouse group that received dmCT was compared with the mice given nCT or mCT E112K as

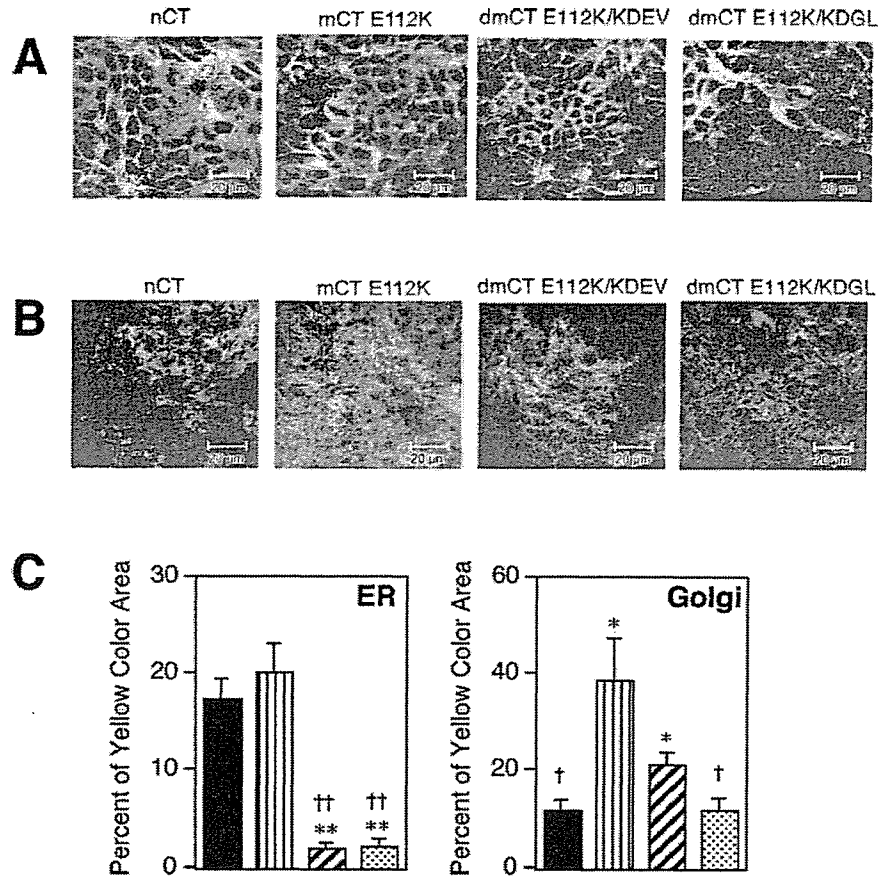

FIGURE 1. Localization of nCT, dmCT E112K/KDEV, dmCT E112K/KDGL, and mCT E112K in T84 cells after incubation. Cells were fixed and analyzed 4 h after the start of Alexa Fluor 488-conjugated nCT, dmCT E112K/KDEV, dmCT E112K/KDGL, and mCT E112K uptake. To identify the intracellular destination, colocalization with ER-Tracker Blue-White *p*-xylene-bis-pyridinium bromide, a marker for the ER, is shown in quasi-red (*A*), whereas BODIPY TR-ceramide, a marker for the Golgi apparatus, is shown in red (*B*). The merged signals appear yellow. Typical image pictures are presented for each group. The yellow color area of nCT (■), mCT E112K (▥), dmCT E112K/KDEV (▨), and dmCT E112K/KDGL (▩) were quantified with ImageJ software (*C*). The values represent the mean ± 1 SEM for six pictures from two different experiments. Each picture covers 12.96 mm^2 of culture surface, which was equal to 262,144 pixels. *, $p < 0.05$; **, $p < 0.01$, when compared with nCT; †, $p < 0.05$; ††, $p < 0.01$, when compared with mCT E112K.

nasal adjuvants using a Mann-Whitney *U* test with StatView II (Abacus Concepts) designed for Macintosh computers. A *p* value of <0.05 or <0.01 was considered significant.

Results

Double mutant CTs fail to track from the Golgi into the ER

Because it has been shown that the COOH terminus of the CT-A subunit KDEL is essential for intracellular movement of CT from the Golgi to the ER, we initially examined intracellular trafficking of our newly developed second generation dmCTs in the T84 human intestinal cell line using confocal microscopic analysis (Fig. 1). After 4 h of incubation, nCT and mCT E112K were detected in the ER of T84 cells (Fig. 1, *A* and *C*, yellow staining); however, dmCT E112K/KDEV and dmCT E112K/KDGL were not detected there (segregated green and red staining; Fig. 1*A*). Thus, the area of yellow staining with both dmCTs was significantly lower than that of nCT and mCT E112K (Fig. 1*C*). Both mCT E112K and dmCT E112K/KDEV were seen in the Golgi apparatus (Fig. 1*B*), and the large area of yellow staining was noted (Fig. 1*C*). Interestingly, the distribution pattern of dmCT E112K/KDEV and dmCT E112K/KDGL differed with the former by being retained longer in the Golgi apparatus than the latter (Fig. 1*B*). Thus, dmCT E112K/KDGL resulted in segregated green and red staining with only a small area of yellow staining (Fig. 1, *B* and *C*). Because a small area of nCT was noted in the Golgi apparatus (Fig. 1*C*), it is

Table I. *Comparison of biologic and toxic activity of mCTs*

Nasal Adjuvant	cAMP Induction[a] (pmol/mg protein)	Y1-Cell Assay[b] (pg/ml)	Ileal Loop Test[c] (W:L ratio)
nCT	104.4 ± 2.3††	0.06 ± 0.01†† (1)[d]	164.3 ± 4.0††
E112K/KDEV	5.3 ± 0.3**	125.0 ± 20.8** (1/2083)	47.7 ± 9.7**
E112K/KDGL	6.5 ± 0.2**	166.7 ± 9.7** (1/2778)	41.7 ± 3.4**
E112K	7.0 ± 1.0**	234.1 ± 44.3* (1/3902)	45.5 ± 0.4**
PBS	7.4 ± 0.5**		37.6 ± 4.4**

[a] CHO cells (1.5×10^4 cells/well) were cultured in F-10 medium containing 1 % FCS with 100 ng/ml of each toxin for 18 h, and the cAMP induction was assessed using an enzyme immunoassay. Values represent the mean ± SEM of nine culture wells in each group. **, $p < 0.01$, when compared with nCT. ††, $p < 0.01$, when compared with mCT E112K.

[b] Y-1 cells were cultured with F-12 medium containing 15% horse serum and 2.5% FCS and serial dilution of each toxin for 24 h. The enterotoxin concentration required to initiate rounding was determined. Values represent the mean ± SEM of of 12 culture wells in each group. *, $p < 0.05$; **, $p < 0.01$, compared with nCT. ††, $p < 0.01$, when compared with mCT E112K.

[c] The ratio of the weight in milligrams to length in centimeters (W:L ratio) after injection of dmCTs into the loop. Each loop was injected with 0.1 ml of 1 μg of dmCTs or nCT. The weight and length of each loop were measured after 3 h values. Values represent the mean ± SEM of six loops in each group. **, $p < 0.01$, when compared with nCT. ††, $p < 0.01$, when compared with mCT E112K.

[d] The values in parenthesis is the ratio of the toxicity of dmCTs to the toxicity of nCT.

Table II. *Comparison of the distribution of dmCTs and nCT in olfactory tissues*

	CNS Tissues					
	ON/E[a]		OBs[a]		ON/E[b]	OBs[b]
Nasal Adjuvants	5 μg	0.5 μg	5 μg	0.5 μg	5 μg	5 μg
nCT	9.61 ± 0.49[†c]	4.03 ± 0.41	1.84 ± 0.55	0.26 ± 0.09	2.23 ± 0.07	1.36 ± 0.02
mCT E112K	3.97 ± 0.37*	4.01 ± 0.65	0.83 ± 0.16	0.12 ± 0.07	1.83 ± 0.19	0.19 ± 0.01**
E112K/KDEV	17.92 ± 1.59*[†]	4.51 ± 0.58	<0.1**[†]	<0.1	0.46 ± 0.14**[†]	<0.1**
E112K/KDGL	14.79 ± 1.07*[†]	4.73 ± 0.37	0.25 ± 0.03**[†]	<0.1	0.39 ± 0.01**[†]	<0.1**

[a] Distribution of acridinium-labeled enterotoxins into the OBs and ON/E was determined 24 h after nasal application of 5 or 0.5 μg of acridinium-labeled nCT, mCT E112K, dmCT E112K/KDEV, or dmCT E112K/KDGL. The OB and ON/E were collected and analyzed for the presence of acridinium-labeled enterotoxin.

[b] Groups of mice were nasally immunized with 100 μg of OVA plus 5 μg of acridinium-labeled nCT, mCT E112K, dmCT E112K/KDEV, or dmCT E112K/KDGL three times at weekly intervals. The distribution of acridinium-labeled enterotoxins in the OBs and ON/E were determined 7 days after the last nasal application. The OBs and ON/E were collected and analyzed for the presence of acridinium-labeled enterotoxin.

[c] Data are expressed as nanograms per 10 mg of tissue ± SEM for nine mice in each experimental group. The CNS tissues of nine mice given nasal PBS were examined for background levels of luminescence. These control values were subtracted from each experimental value. Difference from the value of nCT was statistically significant. (*, $p < 0.05$; **, $p < 0.01$). †, $p < 0.05$, when compared with mCT E112K.

possible that nCT moved quickly into the ER or the surface membrane. In contrast, dmCT E112K/KDGL is most likely redistributed to the surface membrane, because a significantly lower retention signal was found in the ER (Fig. 1*C*). As these results show, because these dmCTs are either retained in the Golgi apparatus (dmCT E112K/KDEV) or redistributed to the surface membrane (dmCT E112K/KDGL), they do not undergo retrograde transport into the ER. In contrast, both nCT and mCT E112K reached the ER within 4 h of incubation.

Enzymatic activity and toxicity of mCTs

The biologic properties and toxicity of dmCTs were examined and compared with those of mCT E112K and nCT (Table I). Essentially no cAMP induction was seen when CHO cells were incubated with dmCTs or mCT E112K. To further examine the toxicity of dmCTs, the morphological changes in Y-1 cells were assessed. Both dmCT E112K/KDEV and E112K/KDGL showed significantly lower toxicity than nCT (1/2083 and 1/2778 of nCT, respectively). In addition, when the mouse ileal loop test was performed to measure toxic manifestations, both dmCTs were found to induce significantly lower levels of fluid accumulation than nCT.

dmCTs do not accumulate in the CNS

To determine whether dmCTs undergo retrograde transport into the CNS, acridinium-labeled dmCT E112K/KDEV, dmCT E112K/KDGL, mCT E112K, or nCT were given by the nasal route. Twenty-four hours after nasal administration of 0.5 μg of nCT, mCT E112K, dmCT E112K/KDEV, and dmCT E112K/KDGL, similar levels of all administered enterotoxins could be detected in the ON/E, but no significant accumulation of the enterotoxins was seen in the OBs (Table II). Accumulation in the ON/E appeared to be dose dependent. Thus, 2- to 4-fold higher quantities of nCT and dmCTs were found in the ON/E after nasal delivery of a 5-μg dose (Table II). At a 5-μg nasal dose, dmCTs accumulated more in the ON/E of mice than did nCT or mCT E112K, but nCT accumulated in the OBs whereas dmCTs did not (Table II). Furthermore, some mCT E112K accumulation was seen in the OBs, although the levels were lower than that of nCT (Table II). The residual levels of dmCT-acridinium compounds in ON/E and OBs were also examined 7 days after the last immunization. Mice were given nasal OVA and acridinium-conjugated nCT, mCT E112K, or dmCTs three times at weekly intervals. Interestingly, no accumulation of either dmCT E112K/KDEV or dmCT E112K/KDGL was detected in the ON/E or the OBs; however, significant amounts of nCT were seen in the OBs (Table II). Furthermore, small amounts of mCT E112K were also detected in the OBs (Table II). Taken together, our studies show that although dmCTs bind and accumulate in the ON/E, these dmCTs do not enter the OBs, whereas nCT quickly traffics into the OBs and remains for at least 7 days after immunization. Furthermore, our findings show that novel dmCTs may have an improved safety profile as nasal adjuvants when compared with mCT E112K, because mCT E112K shows some accumulation in the ON/E and OBs, although the levels were significantly lower than those seen with nCT.

Mucosal adjuvant activity of dmCTs

To assess the mucosal adjuvant properties of dmCTs, the mice were nasally immunized with 100 μg of OVA plus 0.5 μg of dmCT E112K/KDEV, dmCT E112K/KDGL, mCT E112K, or nCT three times at weekly intervals. Plasma and mucosal external secretions (nasal washes, fecal extracts, and saliva) were collected 7 days after the last immunization. Significant levels of OVA-specific S-IgA Ab responses were seen in all external secretions of mice nasally immunized with OVA plus dmCT E112K/KDEV or E112K/KDGL. However, mCT E112K exhibited significantly lower OVA-specific IgA Ab responses in mucosal external secretions than did nCT (Fig. 2). Elevated levels of OVA-specific IgG Ab responses were seen in mice given nasal dmCTs as mucosal adjuvants. OVA-specific IgG Ab responses in mice immunized

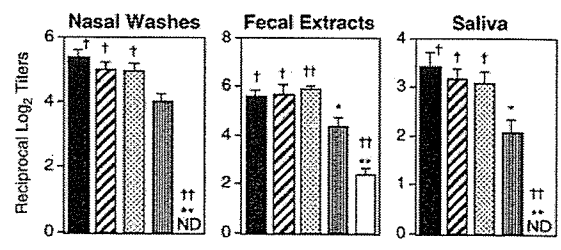

FIGURE 2. Comparison of OVA-specific IgA Ab responses in nasal washes, fecal extracts, and saliva of mice immunized with OVA plus nCT, mCT, or dmCTs. Each mouse group was nasally immunized once a week for three consecutive weeks with 100 μg of OVA plus 0.5 μg of nCT (■), dmCT E112K/KDEV (▨), dmCT E112K/KDGL (▤), mCT E112K (▥), or PBS (□) as mucosal adjuvant. Seven days after the last immunization, the IgA levels in nasal washes and saliva were determined by an OVA-specific ELISA. The values shown are the mean ± 1 SEM for 30 mice in each experimental group. ND indicates that the titer was not detectable. *, $p < 0.05$; **, $p < 0.01$, when compared with nCT; †, $p < 0.05$; ††, $p < 0.01$, when compared with mCT E112K.

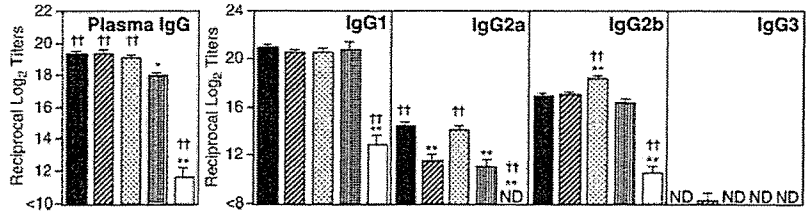

FIGURE 3. Comparison of OVA-specific plasma IgG and IgG subclass Ab responses of C57BL/6 mice nasally immunized with OVA plus nCT, mCT, or dmCTs. Each mouse group was nasally immunized once a week for three consecutive weeks with 100 μg of OVA plus 0.5 μg of nCT (■), dmCT E112K/KDEV (▨), dmCT E112K/KDGL (▨), mCT E112K (▥), or PBS (□) as mucosal adjuvant. Seven days after the last immunization, plasma IgG and IgG subclass Ab levels were determined by OVA-specific ELISA. The values shown are the mean ± 1 SEM for 30 mice in each experimental group. ND, not detected. *, $p < 0.05$; **, $p < 0.01$, when compared with nCT. †, $p < 0.05$; ††, $p < 0.01$, when compared with mCT E112K.

with OVA plus dmCT E112K/KDEV or dmCT E112K/KDGL were identical with those seen in mice given nasal OVA plus nCT (Fig. 3). In contrast, mice given nasal mCT E112K as a mucosal adjuvant showed significant but lower OVA-specific IgG Ab responses than did mice immunized with OVA plus dmCTs or nCT (Fig. 3).

Furthermore, plasma OVA-specific IgG subclass Ab responses were also examined. High levels of OVA-specific-IgG1 and IgG2b Ab responses were seen in mice nasally immunized with OVA plus dmCT E112K/KDEV or E112K/KDGL, as well as in mice given nCT. Although OVA-specific IgG2a Ab responses were relatively lower than those of the IgG1 and IgG2b subclasses, anti-OVA IgG2a titers were significant in mice given nasal nCT or dmCT E112K/KDGL but reduced in those given dmCT E112K/KDEV or mCT E112K. An OVA-specific IgE ELISA revealed elevated levels of OVA-specific IgE Ab responses in plasma of mice given OVA plus nCT (Table III). Most interestingly, significantly lower levels of OVA-specific IgE Abs were noted in mice given nasal OVA plus dmCTs as well as mCT as a nasal adjuvant (Table III).

OVA-specific AFC responses to mCTs

The results of OVA-specific Ab responses were further confirmed at the B cell level by using an OVA-specific ELISPOT assay (Fig. 4). Mononuclear cells from spleens, CLNs, lung, NPs, SMGs, and NALT of mice nasally immunized with OVA plus nCT, mCT E112K, dmCT E112K/KDEV, or dmCT E112K/KDGL were subjected to an OVA-specific ELISPOT assay to determine the numbers and isotypes of AFCs present. In the spleen, CLNs, NPs, and lungs of mice given nasal OVA plus dmCT E112K/KDEV or E112K/KDGL, OVA-specific IgG AFC were elevated to levels comparable to those seen in mice given nCT as nasal adjuvant. In contrast, nasal administration of mCT E112K resulted in levels of anti-OVA IgG AFCs in spleen, CLNs, and lungs that were lower than those seen with dmCTs and nCT. Furthermore, both dmCT E112K/KDEV and dmCT E112K/KDGL induced high numbers of OVA-specific IgA AFCs in NALT, SMGs, and NPs. These results clearly show that the newly developed second generation of dmCT E112K/KDEV and dmCT E112K/KDGL induces Ag-specific Ab responses as effectively as nCT in both systemic and mucosal lymphoid tissues.

Table III. *Comparison of OVA-specific IgE Ab responses induced by nCT, mCT, or dmCTs*

Treatment Group[a]	Ag-Specific IgE[b] (reciprocal $\log_2$ titer)
nCT	7.5 ± 0.3††[c]
E112K/KDEV	3.3 ± 0.4**
E112K/KDGL	3.3 ± 0.3**
E112K	2.3 ± 0.2**
PBS	<2

[a] Each mouse group was nasally immunized once a week for two consecutive weeks with 100 μg of OVA plus 0.5 μg of nCT, mCT E112K/KDEV, mCT E112K/KDGL, mCT E112K, or PBS.

[b] Seven days after the last immunization, OVA-specific IgE levels in plasma were determined by ELISA.

[c] The values shown are the mean ± SEM for 6–8 mice in each experimental group. **, $p < 0.01$, when compared with nCT. ††, $p < 0.01$, when compared with mCT E112K.

OVA-specific CD4$^+$ T cell proliferative and cytokine responses

Because nasal immunization with OVA plus either dmCT E112K/KDEV or dmCT E112K/KDGL induced OVA-specific Ab responses in both systemic and mucosal compartments, it was important to examine the nature of OVA-specific CD4$^+$ Th cell responses. We initially assessed OVA-specific CD4$^+$ T cell proliferative responses in spleen and CLNs of mice nasally immunized with OVA plus dmCTs, nCTs, or mCT E112K. Significantly higher OVA-specific CD4$^+$ T cell proliferative responses were seen in the spleen and CLNs of mice immunized with both dmCT E112K/KDEV and dmCT E112K/KDGL than in mice immunized with mCT E112K (Fig. 5). These OVA-specific CD4$^+$ T cell proliferative responses were comparable to those seen in mice given nCT.

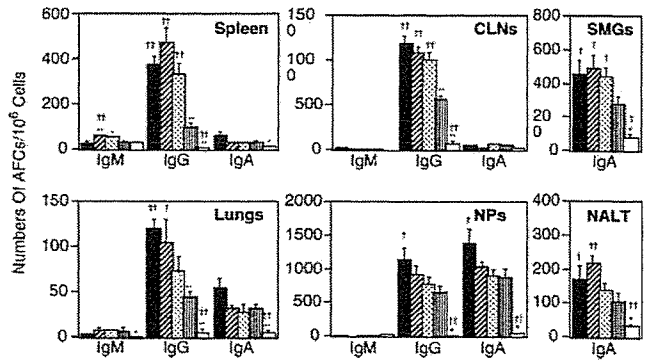

FIGURE 4. Analysis of OVA-specific AFCs in mice immunized nasally with OVA and nCT, mCT, or dmCTs. Each mouse group was nasally immunized once a week for three consecutive weeks with 100 μg of OVA plus 0.5 μg of nCT (■), dmCT E112K/KDEV (▨), dmCT E112K/KDGL (▨), mCT E112K (▥), or PBS (□). Seven days after the last immunization, mononuclear cells isolated from the NPs, SMGs, CLNs, lungs, and spleen were examined using an OVA-specific ELISPOT assay to determine the numbers of IgM, IgG, and IgA AFCs. The results represent the mean values ± 1 SEM for 20 mice in each experimental group. *, $p < 0.05$; **, $p < 0.01$, when compared with nCT. †, $p < 0.05$; ††, $p < 0.01$, when compared with mCT E112K.

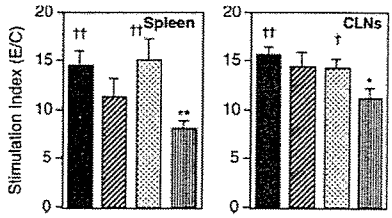

FIGURE 5. Analysis of Ag-specific CD4$^+$ T cell proliferative responses induced by nasal immunization with OVA plus CT derivatives. Each mouse group was nasally immunized once a week for three consecutive weeks with 100 μg of OVA plus 0.5 μg of nCT (■), dmCT E112K/KDEV (▨), dmCT E112K/KDGL (▤), or mCT E112K (▥). The splenic and CLN CD4$^+$ T cells were isolated 7 days after the last immunization and cultured with or without OVA in the presence of APCs. The stimulation index was determined as $A_{450\ nm}$ of wells with OVA divided by wells without OVA (control). The results represent the individual values from three separate experiments. *, $p < 0.05$; **, $p < 0.01$, when compared with nCT; †, $p < 0.05$; ††, $p < 0.01$, when compared with mCT E112K.

We next examined CD4$^+$ Th1- and Th2-type cytokine responses by Ag-specific CD4$^+$ T cells from the spleen and CLNs of mice nasally immunized with OVA plus dmCTs (Fig. 6). Both dmCT E112K/KDEV and dmCT E112K/KDGL induced high levels of Th2-type cytokines (IL-4, IL-5, IL-6, and IL-10) in OVA-stimulated CD4$^+$ T cell cultures. The levels of these cytokines were almost comparable to those seen in OVA-stimulated CD4$^+$ T cells from mice given nCT as nasal adjuvant. Of interest, these Th2-type cytokine responses were comparable to those induced by polyclonal stimulation (solid phase anti-CD3 and anti-CD28 mAb; Fig. 6, dotted lines). In contrast, OVA-stimulated CD4$^+$ T cells from the spleen and CLNs of mice given nasal OVA plus nCT or dmCT E112K/KDGL exhibited similar levels of Th1-type cytokines (IFN-γ and IL-2) (Fig. 6). Although these Th1-type cytokine responses were significantly higher than those responses induced by mCT E112K or dmCT E112K/KDEV as nasal adjuvants, relative Th1-type cytokine production was markedly lower than that induced by anti-CD3 and anti-CD28 mAb stimulation.

Discussion

It is well known that nCT and nLT are effective adjuvants that are capable of enhancing both mucosal S-IgA and systemic IgG Ab responses to coadministered protein Ags in mice and other experimental models. However, both enterotoxins are unsuitable for use in humans due to their toxicity, causing severe diarrhea if given orally and CNS toxicity if administered nasally (14, 15, 42–44). To overcome these obstacles to clinical practicability, several groups, including ours, have focused on developing nontoxic derivatives of CT or LT (10, 16, 17, 45–50). However, although these studies have been successful in producing nontoxic mutants, they did so at times by sacrificing the mucosal adjuvanticity associated with nCT (10, 16, 17, 45–50).

This study shows that a newly developed second generation of dmCTs, which have two amino acid substitutions in the ADP-ribosyltransferase active center (E112K) and COOH-terminal KDEL (dmCT E112K/KDEV or dmCT E112K/KDGL), offer real advantages as nasal adjuvants over the previously developed mCT E112K. When used as nasal adjuvants, even small doses (0.5 μg) of the two dmCTs induced levels of Ag-specific Ab responses in both mucosal and systemic lymphoid tissues that were comparable to those induced by nCT. Unlike nCT, however, that high degree of mucosal adjuvanticity was not accompanied by toxicity. Indeed, both dmCT E112K/KDEV and dmCT E112K/KDGL lacked ADP-ribosyltransferase activity and proved unable to move from the Golgi to the ER. Both dmCTs were thus unable to induce increases in intracellular cAMP. In addition dmCTs did not elicit fluid accumulation in mouse-ligated ileal loops. Furthermore, confocal microscopic analysis showed that the majority of the dmCTs were localized between the surface membranes and the Golgi apparatus

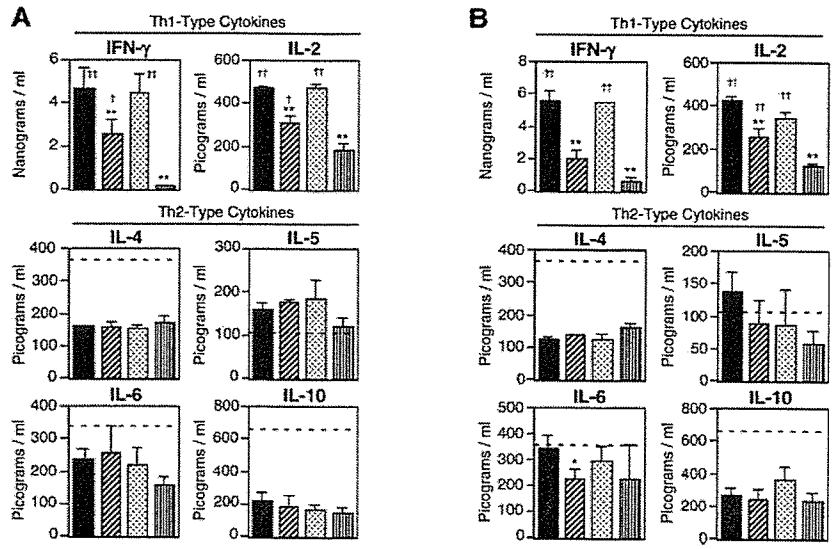

FIGURE 6. OVA-induced CD4$^+$ Th1-type and Th2-type cytokine responses in mice given nasal OVA plus nCT, mCT, or dmCTs. Each mouse group was nasally immunized once a week for three consecutive weeks with 100 μg of OVA plus 0.5 μg of nCT (■), dmCT E112K/KDEV (▨), dmCT E112K/KDGL (▤), or mCT E112K (▥). *A*, The splenic CD4$^+$ T cells (4×10^6 cells/ml) from each mouse group were cultured with 1 mg/ml OVA in the presence of APCs (8×10^6 cells/ml). *B*, The CLN CD4$^+$ T cells (4×10^6 cells/ml) from each mouse group were cultured with 1 mg/ml OVA in the presence of APCs (8×10^6 cells/ml). Culture supernatants were harvested after 5 days of incubation (or after 2 days for IL-2) and analyzed by the respective cytokine-specific ELISA. The dotted lines indicate levels of each cytokine in the wells of anti-CD3 mAb- and anti-CD28 mAb-stimulated CD4$^+$ T cells from spleen or CLNs of naive mice. Th1-type cytokine production by anti-CD3 and anti-CD28 mAb treatments were IFN-γ at ~80 ng/ml and IL-2 at ~10 ng/ml, respectively. The values shown are the mean ± SEM of 15 mice in each group. *, $p < 0.05$; **, $p < 0.01$, when compared with nCT; †, $p < 0.05$; ††, $p < 0.01$, when compared with mCT E112K.